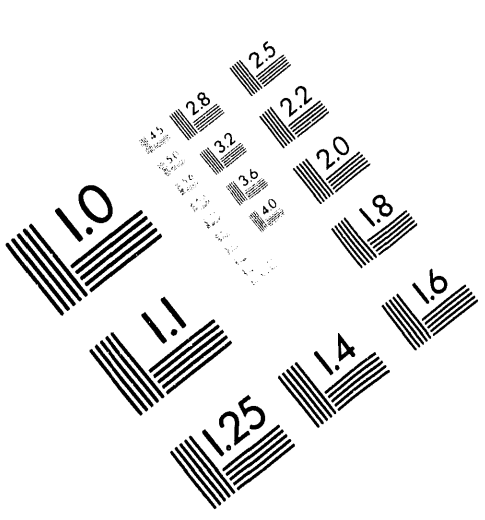

Association for Information and Image Management

1100 Wayne Avenue, Suite 1100
Silver Spring, Maryland 20910

301/587-8202

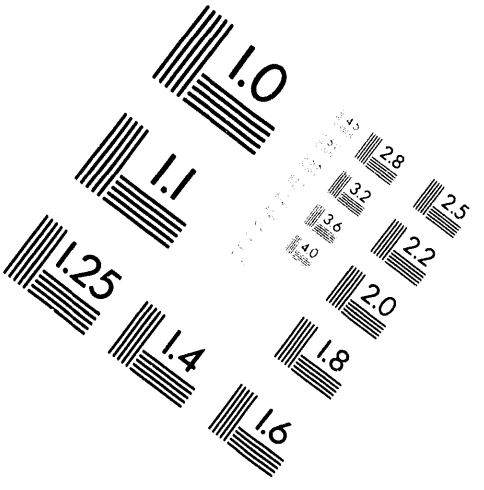

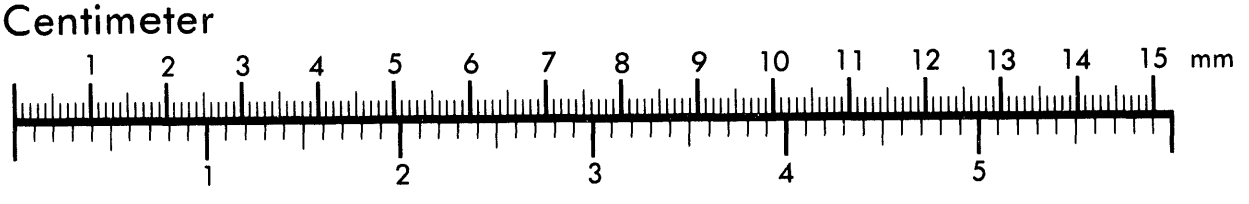

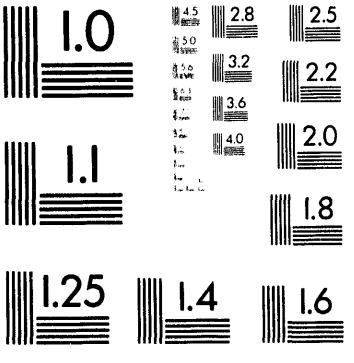

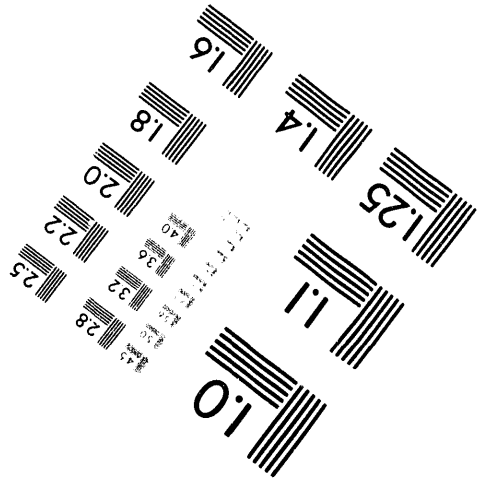

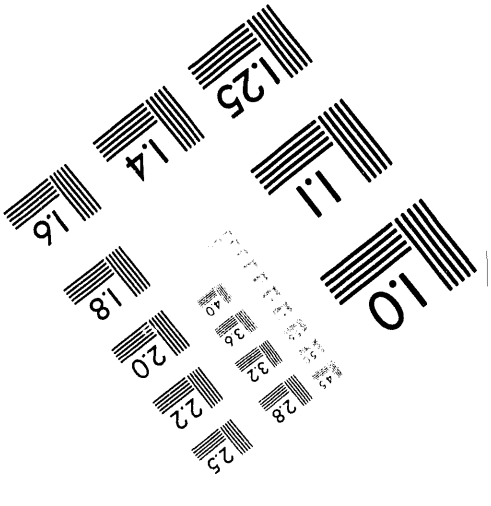

MANUFACTURED TO AIIM STANDARDS
BY APPLIED IMAGE, INC.

1 of 1

ORNL/HTSPC-5

ORNL SUPERCONDUCTING TECHNOLOGY PROGRAM FOR ELECTRIC POWER SYSTEMS

ANNUAL REPORT FOR FY 1993

Compiled by
R. A. Hawsey

Manuscript Completed—February 1994
Date Published—April 1994

Prepared for the
Advanced Utility Concepts Division
Office of Energy Management
Office of Utility Technologies
Office of Energy Efficiency and Renewable Energy
U.S. DEPARTMENT OF ENERGY
(AK 06 00 00 0)

Prepared by
OAK RIDGE NATIONAL LABORATORY
P.O. Box 2008
managed by
MARTIN MARIETTA ENERGY SYSTEMS, INC.
for the
U.S. DEPARTMENT OF ENERGY
under contract DE-AC05-84OR21400

CONTRIBUTORS

J. Brynestad
J. D. Budai
R. Chou[1]
D. K. Christen
J. S. DeLuca[2]
L. Dresner
A. Goyal
R. A. Hawsey
H. Hsu[3]
T. T. Kodas[4]
D. R. James
C. J. Janke
D. M. Kroeger
R. J. Lauf
D. H. Lowndes
F. A. List
M. S. Lubell
J. W. Lue
B. W. McConnell
H. E. McCoy
R. W. Murphy
D. P. Norton
M. Paranthaman[5]
S. W. Schwenterly
V. Selvamanickam[5]
V. K. Sikka
E. D. Specht
J. A. Sutliff[2]
J. E. Tkaczyk[2]
J. R. Thompson
Z. L. Wang[6]
R. K. Williams
C. B. Zimm[7]

[1]Lehigh University
[2]General Electric Corporate Research and Development
[3]Consultant
[4]University of New Mexico
[5]Postdoctoral research Fellow
[6]University of Tennessee
[7]Astronautics Corporation of America

CONTENTS

Page

LIST OF FIGURES v

LIST OF TABLES ix

ACRONYMS AND INITIALISMS xi

EXECUTIVE SUMMARY xiii

TECHNICAL PROGRESS IN HIGH-TEMPERATURE SUPERCONDUCTOR WIRE DEVELOPMENT 1-1
- CRITICAL CURRENTS AND MICROSTRUCTURES OF HIGH-TEMPERATURE SUPERCONDUCTOR MATERIALS 1-1
  - Local Texture and Percolative Paths for Strongly Linked Current Flow in Spray-Pyrolyzed $TlBa_2Ca_2Cu_3O_{8+x}$ Deposits 1-1
  - Y-Ba-Cu-O Wires with Reduced Weak-Link Behavior 1-11
- Tl-1223 POWDER-IN-TUBE CONDUCTOR FABRICATION AND PROCESSING 1-14
- BSCCO POWDER-IN-TUBE AND DEPOSITED CONDUCTOR DEVELOPMENT 1-19
  - Powder-in-Tube 1-19
  - Deposited Conductor Development 1-23

TECHNICAL PROGRESS IN APPLICATIONS DEVELOPMENT 2-1
- DEMONSTRATION OF A MAGNETIC REFRIGERATOR FOR HIGH-TEMPERATURE SUPERCONDUCTOR DEVICE APPLICATIONS 2-1
  - Approach 2-1
  - Results 2-2
  - FY 1994 Plans 2-4
- HIGH-TEMPERATURE SUPERCONDUCTOR COIL DEVELOPMENT FOR ELECTRIC POWER APPLICATIONS 2-4

SUMMARY OF TECHNOLOGY TRANSFER ACTIVITIES 3-1
- BACKGROUND 3-1
- RELATIONSHIP TO THE DOE MISSION 3-1
- FUNDING 3-2
- TECHNOLOGY TRANSFER APPROACH 3-2
- PROGRAM MEASURES 3-7
- PROGRAM HIGHLIGHTS 3-7
  - Licensing of Superconducting Wire Technology 3-7
  - Nanoindenter at ORNL's High-Temperature Materials Laboratory . . . 3-9
  - Publications and Presentations 3-9

FY 1993 PUBLICATIONS AND PRESENTATIONS 4-1

LIST OF FIGURES

Figure		*Page*
1.1	The volume pinning force density $F_p = J_c \times B$ for a series of four (*a*) unirradiated and (*b*) irradiated Tl-1223 thick films	1-2
1.2	The irreversibility lines B_{irr} (T) for heavy-ion irradiated materials: Tl-1223 textured thick films, and YBCO and Bi-2212 single crystals	1-3
1.3	Properties of Tl-1223 deposits before and after heat treatment at 600°C in oxygen	1-4
1.4	Transmission electron microscopy cross-section image showing the substrate, a thin reaction layer, and tilt (perpendicular to the substrate) and twist (parallel to the substrate) grain boundaries	1-5
1.5	Intensity distribution for X-ray diffraction azimuthal scans using (*a*) wide and (*b*) narrow X-ray beams	1-6
1.6	Electron backscatter diffraction pattern measurements indicating the structure within a single colony	1-7
1.7	Electron backscatter diffraction pattern measurements indicating the structure at a colony intersection	1-8
1.8	Electron backscatter diffraction pattern measurements of another colony intersection	1-8
1. 9	Angular positions of peaks in X-ray diffraction azimuthal scan intensity distributions obtained using a narrow 100-μm-diam beam as a function of position along the gage length	1-9
1.10	The *apparent* critical current density of a Tl-1223 deposit as a function of the sample width as the same sample was progressively patterned to narrower conductance bridge widths	1-10
1.11	American Superconductor's Y-124 conductor prepared by oxidation of the metallic precursor	1-12
1.12	Typical morphology of aerosol powders that convert to the Tl-1223 phase in powder-in-tube form	1-15
1.13	Thermal analysis of power-in-tube $Tl_{0.8}Ba_{1.9}Ca_{2.0}Cu_{3.0}Ag_{0.35}O_x$	1-16
1.14	Typical processing schedule for aerosol powders	1-16

Figure		*Page*
1.15	Typical resistive transition	1-17
1.16	Typical variation of the critical current density at 77 K	1-17
1.17	Morphology of peeled tapes	1-18
1.18	Critical current at zero-field plotted as a function of sintering temperature	1-19
1.19	Lower J_c samples reflecting a small peak effect	1-21
1.20	Aerosol pyrolysis system	1-22
1.21	Typical load-displacement curve consisting of a single loading cycle	1-24
1.22	Typical load-displacement curve	1-25
2.1	The solid state cooling process used in magnetic refrigeration	2-2
2.2	Active magnetic regenerator	2-3
2.3	Test results from use of primary magnetocaloric material (7 T, 15 atm) in the Active Magnetic Regenerator Universal Test Apparatus	2-3
2.4	Level and size map for cryocoolers	2-4
2.5	High-temperature superconductor coil	2-5
2.6	*n*-value as a function of external field: (*a*) Y-124 coil; (*b*) Bi-2223 coil	2-6
2.7	Critical current as a function of magnetic field at different temperatures for a small coil made of Y-124 superconductor by American Superconductor Corporation	2-6
2.8	Critical currents as a function of magnetic field at different temperatures of a small solenoid coil made of Bi-2223 superconductor by American Superconductor Corporation.	2-7
2.9	Intermagnetics General Corporation coil test results (No. 3, n vs B)	2-7
2.10	Intermagnetics General Corporation coil test results (No. 3, I_c vs T)	2-8
2.11	Temperature rise due to eddy current heating in ramped fields of 2.5 T/s (not significant in operating area of interest 4.2 K or above 20 K)	2-8

Figure *Page*

3.1 ORNL funding distribution: FY 1993 new budget authorization and outlay . . 3-6

3.2 FY 1993 publications and presentations 3-9

LIST OF TABLES

Table		*Page*
1.1	Heat treatment results on a superplastically deformed 75% Y-123–25% silver sample	1-14
1.2	Effect of heat treatment temperature (short heat treatments)	1-18
1.3	Effect of heat treatment time at optimum temperature	1-20
1.4	Effect of heat treatment temperature (long heat treatments)	1-20
1.5	Mechanical properties of BSCCO powder-in-tube samples	1-25
3.1	Superconducting Technology Program funding: authorization and outlay	3-2
3.2	Summary of funds-out cooperative agreements: January 31, 1994	3-3
3.3	Superconducting Technology Program invention disclosures	3-8

ACRONYMS AND INITIALISMS

ASC	American Superconductor Corporation
CIP	cold isostatic pressing
CRADA	cooperative research and development agreement
CTE	coefficient of thermal expansion
DOE	U.S. Department of Energy
DOE-HQ	DOE Headquarters
EBSP	electron backscatter diffraction patterns
EPRI	Electric Power Research Institute
HIP	hot isostatic pressing
IGC	Intermagnetics General Corporation
MPM	mechanical properties microprobe
ORNL	Oak Ridge National Laboratory
PIT	powder-in-tube
REC	Reliance Electric Company
SCI	Superconductive Components, Inc.
SEM	scanning electron microscopy
TEM	transmission electron microscopy

Executive Summary

The Oak Ridge National Laboratory (ORNL) Superconducting Technology Program is conducted as part of a national effort by the U.S. Department of Energy's Office of Energy Efficiency and Renewable Energy to develop the technology base needed by U.S. industry for commercial development of electric power applications of high-temperature superconductivity. The two major elements of this program are conductor development and applications development. This document describes the major research and development activities for this program together with related accomplishments. The technical progress reported was summarized from information prepared for the FY 1993 Annual Program Review held July 28–29, 1993. This ORNL program is highly leveraged by the staff and other resources of U.S. industry and universities. In fact, nearly three-fourths of the ORNL effort is devoted to industrial competitiveness projects with private companies. Interlaboratory teams are also in place on a number of industry-driven projects. Patent disclosures, working group meetings, staff exchanges, and joint publications and presentations ensure that there *is* technology transfer to U.S. industry. Working together, the collaborative teams are making rapid progress in solving the scientific and technical issues necessary for the commercialization of long lengths of practical high-temperature superconductor wire and wire products.

Technical Progress in High-Temperature Superconductor Wire Development

CRITICAL CURRENTS AND MICROSTRUCTURES OF HIGH-TEMPERATURE SUPERCONDUCTOR MATERIALS

Local Texture and Percolative Paths for Strongly Linked Current Flow in Spray-Pyrolyzed $TBa_2Ca_2Cu_3O_{8+x}$ Deposits

Deposits of $TBa_2Ca_2Cu_3O_{8+x}$, prepared at General Electric Company by vapor-phase thallination of spray-pyrolyzed precursor deposits on polycrystalline yttria-stabilized zirconia substrates, have been shown to have excellent critical current density behavior in high fields at high temperatures.[1,2] The deposits are polycrystalline and have small grains with excellent *c*-axis alignment. Resistively measured critical current density, J_c, as high as 3×10^5 A/cm^2 at 77 K in zero field has been obtained, and at 60 K values remain well above 10^4 A/cm^2 in a 1-T field applied parallel to the *c* axis. In studies of deposits containing columnar defects resulting from heavy-ion irradiation, we have shown that, with optimal defect densities, the irreversibility field at 77 K is in the range reported for $YBa_2Cu_3O_7$. These results indicate the great promise of Tl-1223 deposits for high-field conductor applications at high temperatures.

In as-grown films, J_c vs H curves for H parallel to the *c* axis typically decrease by a factor of 3 to 5 at 0.01 T, and at higher fields they exhibit an extended plateau. This field dependence indicates that the sample contains parallel weakly and strongly linked current paths. We have conducted extensive characterization studies directed toward determining the limitations on J_c and what aspects of the microstructure lead to the strongly linked paths. Heavy-ion irradiations and thermal annealing were correlated with J_c enhancements that could be attributed to a strong-linked component. Transmission electron microscopy (TEM), electron backscatter diffraction, and X-ray microdiffraction were used to define colonies of grains with similar but not identical *a*-axis orientations. Within a colony, *c*-axis tilt grain boundaries have small misorientation angles and thus are not expected to be weak links. It is proposed that long-range current flow is through a percolative network of small-angle boundaries at colony intersections. Electrical transport properties measured on films with progressively narrower conduction bridges confirm this view.

Experimental

Samples were prepared according to procedures described previously.[1,3] Film thicknesses were ~3 μm. Zero field J_c's at 77 K were measured with an electric field criterion of 1 μV/cm on a bridge pattern etched from the film. Typical bridge dimensions were 4 x 0.2 mm or 3 × 0.1 mm. In some cases voltage connections at 1-mm intervals were along the bridge, permitting measurement of J_c in each of four 1-mm segments. In such cases J_c varies by as much as a factor of 3 or 4 from segment to segment.[1] The heavy-ion irradiations were conducted at the Oak Ridge National Laboratory (ORNL) Holifield Accelerator Facility where the samples were bombarded parallel to the *c* axis with 580-MeV Ag^{30+} ions. The resulting amorphous, columnar defects are nearly optimal flux-pinning defects. Microstructural information regarding grain morphology and grain-boundary chemistry and misorientation was obtained using scanning electron microscopy (SEM) and TEM. Local texture information

was inferred from X-ray diffraction measurements, TEM, and electron backscatter diffraction patterns (EBSP). This last technique provides Kikuchi diffraction patterns formed by backscattered electrons in a scanning electron microscope. Spatial resolution was ~1000 Å. Because grain sizes in the basal plane were in the range of 3 to 0 μm, these patterns could be analyzed to obtain the orientations of individual grains at the surface of the film.

Results

Heavy ion irradiation. Electrical transport measurements and analysis of several samples were compared both before and after heavy-ion irradiations. The findings are summarized as follows:

- The materials have a weak-link component that shows marked field sensitivity at low fields. This component is nominally degraded by the irradiation damage.
- At higher fields ($H > 1$ T), J_c is limited by intragrain properties of a strong-linked component and is substantially enhanced after irradiations to a dose of 2.4×10^{11} ions/cm^2 (which corresponds to a defect track areal density that approximately matches the vortex density at $B_\phi \approx 5$ T).
- After irradiation the irreversibility line is raised by 20 K.
- When properly scaled to account for differences in the amount of weak-linked component among different samples, the data fall on separate, universal curves representative of properties before and after irradiation.

To illustrate these observations, Fig. 1.1(*a*) shows the volume-pinning force density $F_p = J_c \times B$ at 77 K for four samples representing properties before and after irradiation. Fig. 1.1(*b*) illustrates that, after scaling to the maximum $F_{p,max}$, the samples

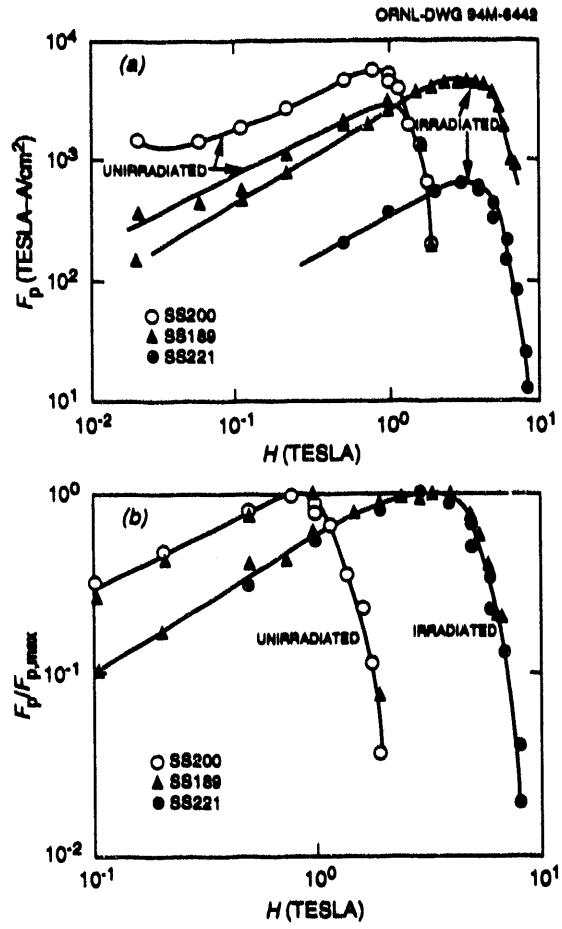

Fig. 1.1. The volume pinning force density $F_p = J_c \times B$ for a series of four (*a*) unirradiated and (*b*) irradiated Tl-1223 thick films. Note that the best as-grown film, SS200, was never irradiated. The other films have larger and varying fractions of weak-linked component. However, when scaled by the maximum pinning force density $F_{p,max}$, the data of Fig. (*b*) fall onto two "universal" curves: one that is characteristic of the as-formed material and one that is characteristic of the pinning-enhanced, irradiated material.

exhibit distinctly different but universal behaviors that are characteristic of the materials in the unirradiated and irradiated states. Moreover, the irreversibility field has been extended from about 2 T in the unirradiated samples to 6 to 7 T in the irradiated samples. Although the absolute values vary among samples, the data suggest reproducible properties and enhancements in the strong-linked component of the material,

while this well-connected component represents only a small fraction (i.e., 1 to 10%) of the sample.

Figure 1.2 shows enhancements in the irreversibility lines obtained by heavy-ion irradiations of the Tl-1223 films along with previous results obtained on Bi-2212 and YBCO single crystals. Note that fluences corresponding to an equivalent flux density $B_\phi \approx 5$ T have been found to produce near-optimal defects for BSCCO and YBCO. The larger relative increases, yet smaller overall values, of B_{irr} for BSCCO compared with YBCO have been ascribed to intrinsic effects of weak flux lattice rigidity resulting from the much larger electronic anisotropy, which results in weaker interplanar coupling. The results for Tl-1223 are encouraging and may have technological significance. The data show both large increases and high values together with the added benefit of a higher $T_c \approx 105$ K. In the high-temperature (liquid nitrogen) regime the flux-pinning defects have enhanced B_{irr} from values below those of YBCO to values that exceed the upper critical field of YBCO for temperatures above 90 K. Apparently, B_{irr} (T) will cross that of YBCO somewhere below 77 K, indicating anisotropy in the Tl-1223 system that lies intermediate between YBCO and Bi-2212. The data on three different films show reproducibility in the effects.

Thermal annealing effects. Although a significant weak-linked component is evident in these materials, the superconductive transport properties at fields above a few tenths of a tesla appear to be limited by intragranular effects, implying a network of strongly coupled grains. An interesting and consistent property of these deposits is an enhancement in J_c that is produced by a postformation anneal at 600°C in oxygen. This annealing effect could arise from improvements in the volume fraction of well-connected material, from a fundamental enhancement in the electronic properties, or from both. We have conducted experiments on two of these as-grown films to correlate the effects of the 600°C thermal-processing step on J_c, the normal state resistivity, and on the Hall carrier density $n_H = 1/R_H e$. Measurements of these transport properties before and after the anneal are illustrated in Fig. 1.3 for one of the two films (the results were confirmed

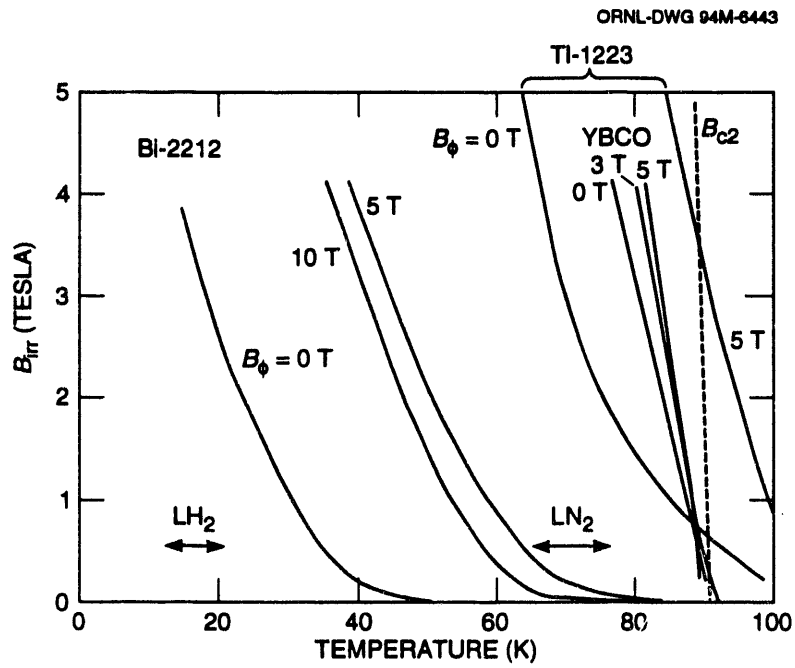

Fig. 1.2. The irreversibility lines B_{irr} (T) for heavy-ion irradiated materials: Tl-1223 textured thick films, and YBCO and Bi-2212 single crystals. All data are taken with the field parallel to the *c* axis, and the temperature ranges of pumped liquid hydrogen and liquid nitrogen are indicated.

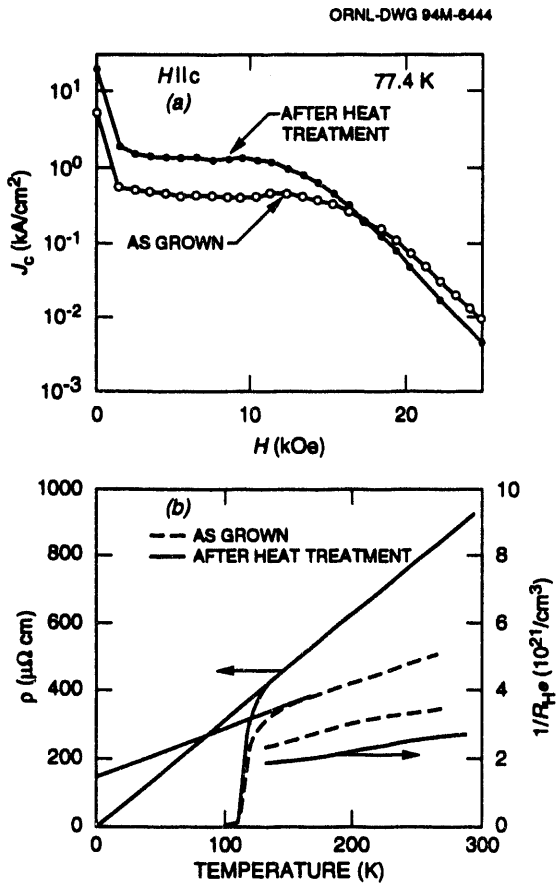

Fig. 1.3. Properties of Tl-1223 deposits before and after heat treatment at 600°C in oxygen: (*a*) field dependence of the critical current density at 77 K (the low-field J_c is increased, but the high-field J_c and the irreversibility field are decreased); (*b*) the normal state resistivity and Hall electronic carrier density (changes in both phenomena imply a reduction in Hall carrier density).

for both films). The figure illustrates typical enhancements by a factor 3 to 4 in the low-field J_c at 77 K. However, at fields above about 1.7 T, J_c is diminished, and the irreversibility field is reduced by about 0.3 T after the anneal. This crossover with field seems to exclude effects due only to geometrical improvements (better grain connectivity). Indeed, the results of normal state transport properties shown in the figure reveal both an approximate 30% increase in the electrical resistivity and reduction in the apparent hole-like Hall carrier density. Although this effect could arise from a loss of well-connected normal state material, the overall temperature dependence of ρ (T) has been modified as evidenced by extrapolations of the linear portions. In addition, close inspection of the resistive transition shows a sharpening of the transition accompanied by some loss of a high-temperature (115 K) component, which could indicate effects of residual-phase conversion. Overall, the observations imply a likely combination of both geometrical and electronic modifications due to the heat treatment as follows:

- The volume fraction of connected grains in the superconductive state has increased. This would explain the overall factor of 3 upward scaling of J_c at low fields (i.e., an approximately constant shift on a log scale).
- The electronic hole carrier density has decreased. This is consistent with the increase in normal state resistivity and decrease in apparent Hall carrier density.
- Modifications in electronic properties through phase changes also could be related to the changes in temperature dependence of ρ and the sharpening of the resistive transition. Moreover, a reduction in carrier concentration n should decrease the energy of pre-existing flux-pinning defects, according to $\Delta U/U \propto \Delta n/n$, which is qualitatively consistent with the observed decrease in the irreversibility field.

Compared with epitaxial films, the overall scale of J_c in these deposits suggests that less than 10% of the material is transporting strong currents in the superconducting state, while a much larger fraction is effectively active with respect to normal state properties. For this reason, direct linkage between changes in normal state and superconductive phenomena may be

difficult to evaluate. The observations of these studies must be closely correlated with ongoing investigations of the microstructure and its modification after such thermal treatment (see "Microstructural characterization").

Microstructural characterization. Figure 1.4 shows a TEM image of a cross-section specimen in which both twist boundaries (parallel to the basal plane) and tilt boundaries (approximately perpendicular to the basal plane) are seen. Alignment of the *c* axis perpendicular to the substrate surface is seen to be good. SEM images of fracture surfaces and EBSP measurements (discussed in the following paragraphs) indicate that basal plane dimensions of grains are in the range of 3 to 10 μm. TEM images indicate that in the *c* direction, grain thicknesses tend to range from 0.5 to 2 μm. Aspect ratios are thus ~ 10—intermediate between those in Y-123 and Bi-Sr-Ca-Cu-O. The average thickness of the deposit is ~ 3 μm such that in most areas it is only a few grains thick. Examination of a number of images suggests that perpendicular boundaries tend, in association with short segments of parallel boundaries, to extend through the thickness of the deposit (see arrows in Fig. 1.4). Composition determinations at edge-on twist boundaries from energy-dispersive electron spectroscopy indicate thallium enrichment compared with the bulk. High-resolution images suggest that this nonstoichiometry results from the nature of the grain termination at the boundary rather than a grain-boundary phase. Thallium enrichment at *c*-axis twist boundaries is significantly enhanced by the post-thallination treatment in oxygen at 600°C, which has been found to increase J_c by a factor of 3 to 4.

Fig. 1.4. Transmission electron microscopy cross-section image showing the substrate, a thin reaction layer, and tilt (perpendicular to the substrate) and twist (parallel to the substrate) grain boundaries. As indicated by the arrows, tilt boundaries tend, in combination with short segments of twist boundary, to extend over several grains. The thin area in this view covers about half the sample thickness.

Misorientation angles for 20 grain boundaries were derived from convergent beam electron diffraction patterns for grains on either side of the boundary. Of eleven *c*-axis twist boundaries, ten had misorientation angles less than 10°, and five of nine tilt boundaries had misorientation angles under 15°. This is a small sample, but the results

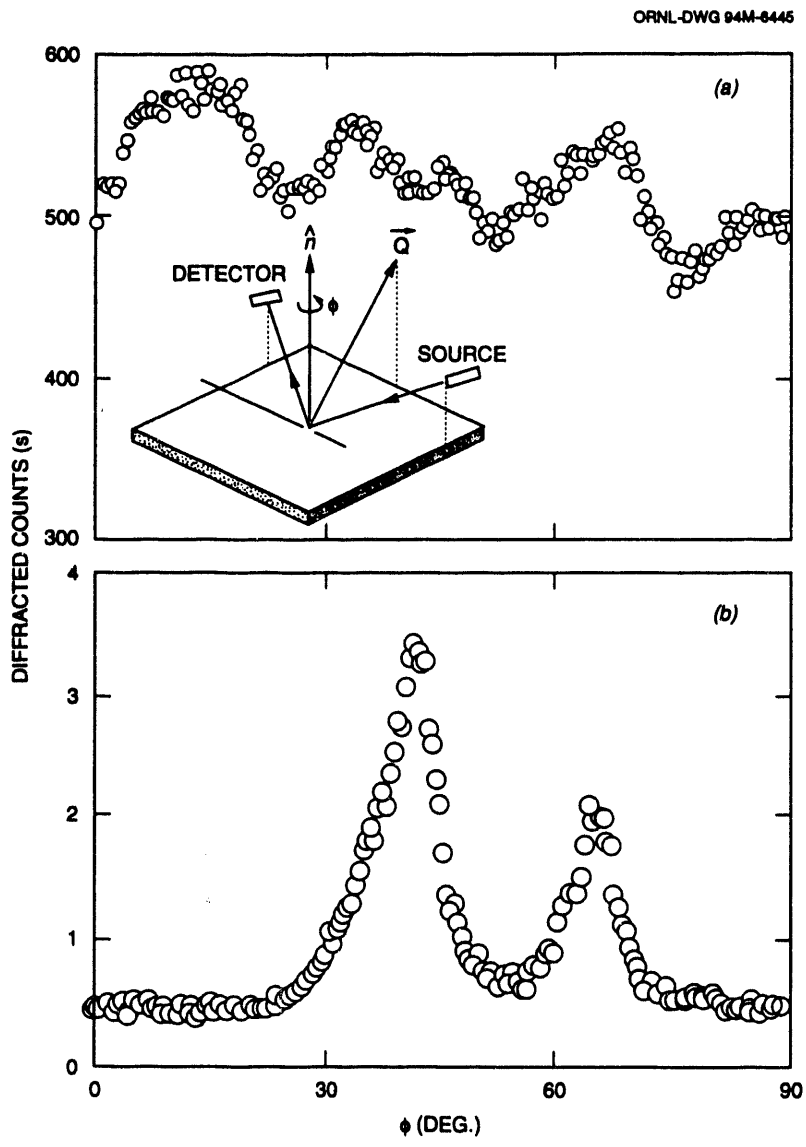

Fig. 1.5. Intensity distribution for X-ray diffraction azimuthal scans using (*a*) wide and (*b*) narrow X-ray beams.

The presence of local texture was confirmed by X-ray diffraction azimuthal scans using large and small X-ray beams. Figure 1.5 shows two X-ray diffraction azimuthal scans of the same deposit using a large beam that illuminated approximately half the sample including one of the 4 × 8 mm current tabs and a small beam that was ~0.5 mm in diam. The positions of the source and detector, along with the axis of rotation of the sample, are indicated. The detector was positioned to detect a non-(00ℓ) peak. Since the deposit has good *c*-axis alignment, the intensity at a given angle ϕ is proportional to the fraction of the deposit area illuminated by the beam, which had some specific basal plane orientation. Thus the ϕ scans of Fig. 1.5 are, effectively, distribution plots for the directions of the *a* axes of grains relative to a fixed arbitrary angle.

Figure 1.5(*a*) indicates the intensity of the (103) reflection as a function of rotation about the film normal (i.e., the *c* axis) using the wide beam. The intensity distribution consists of several peaks superimposed on an average intensity that is well above background. These data suggest that basal plane orientations of grains are largely random but that there is a tendency for clustering around several specific directions. This result is consistent with previous EBSP measurements of the orientations of a large number of grains at

do not appear to be consistent with a previous conclusion (from EBSP determinations of the orientations of a large number of grains at widely separated positions on the sample surface) that the basal plane orientations are random.[4] Taken together, the two results suggest the presence of local texture in which adjacent grains tend to have similar orientations, even though macroscopically all orientations are present in similar numbers.

random locations. However, a very different intensity distribution was obtained when a narrow X-ray beam was used, indicating that, locally, grains are far from randomly oriented. Figure 1.5(*b*) shows an azimuthal scan of the (10$\underline{1}$0) reflection obtained with a narrow beam that had a projected area on the sample of ~ 0.5 × 1 mm. The intensity distribution shows two strong peaks with a low intensity (near background) at all other angles, indicating that basal plane orientations for grains within the illuminated area cluster strongly around only two directions. For approximately 20 such local scans obtained on separate areas of two different deposits, the number of peaks ranged from 1 to 5. These results indicate that, although over the whole deposit many basal plane orientations occur, there is a high degree of local texture indicative of the presence of colonies of grains with similar orientations.

The presence of colonies of grains with similar *a*-axis orientations was confirmed using electron backscatter diffraction. Diffraction patterns were obtained from a large number of points within a rectangular area on the sample surface that had been lightly polished to remove silver and secondary-phase particles. While the diffraction pattern was observed, the electron beam was moved in a line over the sample surface. When a shift in the pattern was noted, the new pattern was recorded and analyzed to obtain the local crystalline orientation. Since the *c* axes are very well aligned, the orientation can be represented by a single arrow in the *a* direction. In Fig. 1.6, the *a*-axis directions are plotted for a 40 × 120 μm area. The beam was moved along parallel lines separated by 12 μm to obtain data over the rectangular grid. An arrow is plotted only where a shift in diffraction pattern was seen (i.e., at a grain boundary). The spacing between arrows is roughly indicative of grain size (although surface irregularities prevented obtaining patterns in some areas, and therefore some

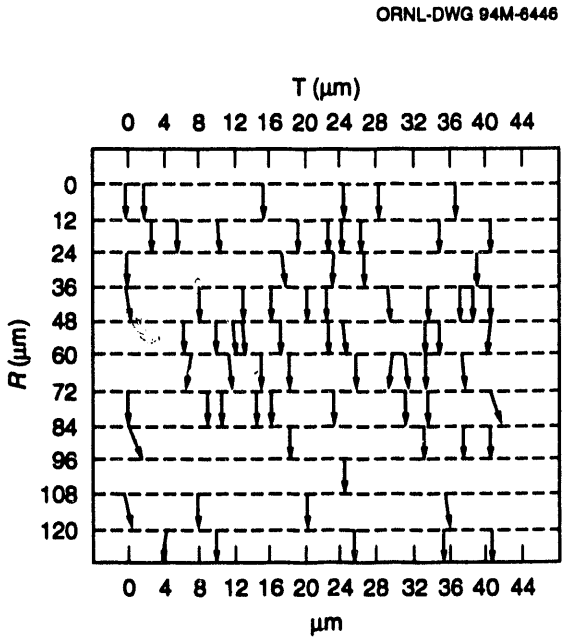

Fig. 1.6. Electron backscatter diffraction pattern measurements indicating the structure within a single colony. The arrows represent the direction of the *a* axis of the grains. The *c* axis is normal to the substrate.

shifts in orientation were missed). Clearly this area is within a single colony. The total spread in *a*-axis orientation is ~ 15 to 20°. Figure 1.7 shows a similar map over a somewhat larger area of the same sample. In this case an irregularly shaped colony intersection can be discerned clearly. The average *a*-axis orientations of the two colonies differ by ~ 35 to 40°. Note that the misorientation across the colony intersection is not constant. Figure 1.8 shows an EBSP map of another colony intersection. In this case a gradual change of orientation can be seen across the intersection; hence, the colony boundary is not easily discerned.

The variation in the number of colonies and their orientations over the length of the patterned bridge was obtained from a series of synchrotron X-ray diffraction azimuthal scans taken at 0.5-mm intervals. The results are shown in Fig. 1.9. The angular positions of X-ray diffraction peaks from plots

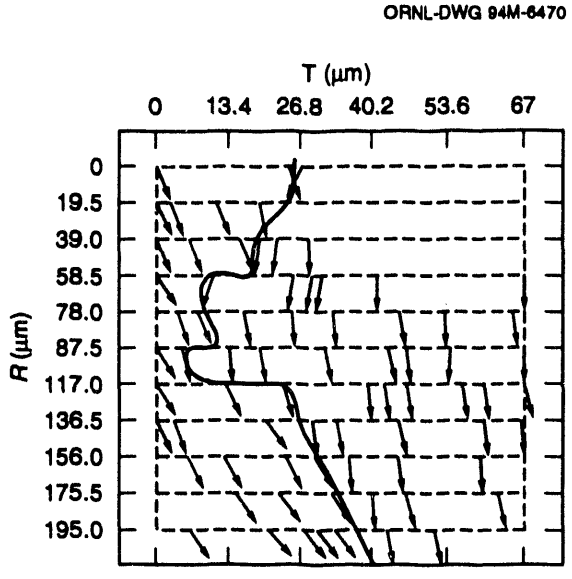

Fig. 1.7. Electron backscatter diffraction pattern measurements indicating the structure at a colony intersection. Many high-angle boundaries are formed at the intersection.

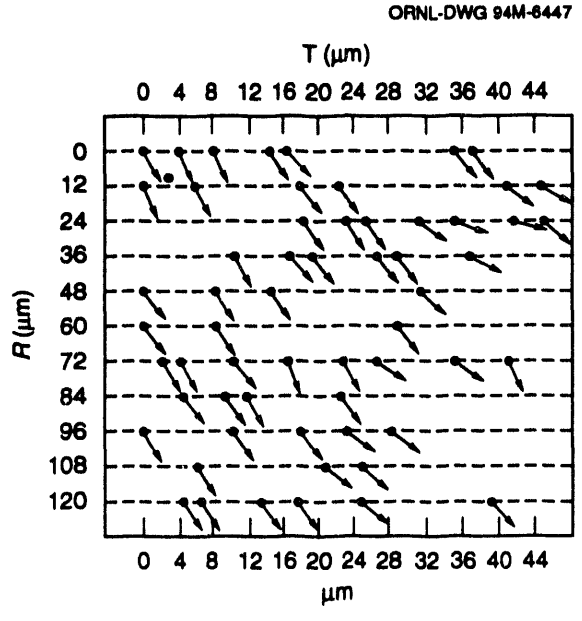

Fig. 1.8. Electron backscatter diffraction pattern measurements of another colony intersection. A gradual change or orientation across the intersection from one colony to another can be seen.

obtained using a 100-μm-diam beam are plotted as a function of position along the gage length. The measured J_c's for each of the four sections are indicated. Although particular a-axis orientations (presumably indicative of colonies of grains of similar orientation) arise and disappear as a function of position, a small-angle boundary connection usually is evident within segments that have a high J_c. The results for this particular sample suggest that, within the gage length, there may be only three or four colonies with a tendency for colony orientations to be correlated locally. The lowest J_c segment manifests the weaker connection owing to a large and abrupt change in intercolony orientation.

Correlations with sample width. Within these identified grain colonies, which can be up to ~ 1 mm in size, a high degree of local texture exists in which a-axis grain orientations are distributed over an angular range of ~ 10 to 15°. Current conduction within these colonies is relatively effective, since current flow can occur across arrays of low-angle, basal plane tilt boundaries. Overall limitations on J_c apparently occur because of transport across the interface between adjacent colonies, which in general can have mean orientations that differ by up to ±45° (owing to the tetragonal crystal symmetry). These limitations likely arise from a reduced fraction of low-angle percolative paths in the interface region, where these paths exist owing to overlap in the distributions of adjacent colony grain-boundary angles. In view of this proposed mechanism, the electrical coupling between adjacent colonies is crucially sensitive to their random relative misorientation.

Several features that have been observed in the transport properties could likely arise in part from the relative sample and colony dimensions. As is described above, in normal practice electrical transport measurements are performed on films that have been patterned to conduction bridges having typical dimensions of 100 to 200 μm wide by 3 to 4 mm long. Therefore the small lateral bridge size should limit current path

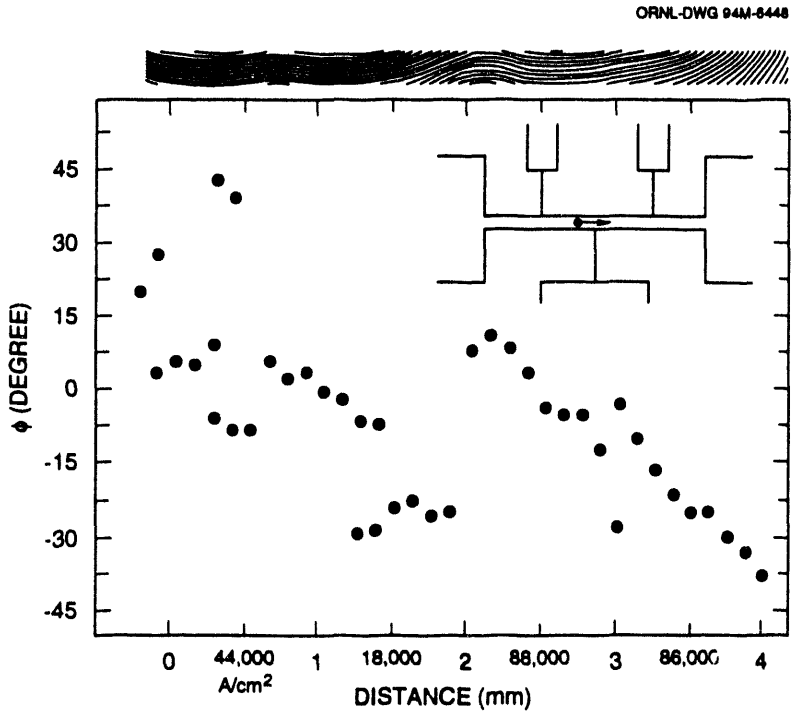

Fig. 1.9. Angular positions of peaks in X-ray diffraction azimuthal scan intensity distributions obtained using a narrow 100-μm-diam beam as a function of position along the gage length. The J_c values for each 1-mm-long bridge segment are indicated. The bar at the top traces the best-connected paths by indicating the local in-plane *a*-axis orientation.

options to a series of one or more single colony boundaries along the bridge length. This hypothesis is consistent with the following observations:

- There is wide variability in the observed J_c of different patterned films and in different segments along the bridge length of the same film.
- The dependence of J_c on magnetic field is similar for different films despite the wide variability in its magnitude.
- Introduction of the tailored defect structures (such as heavy-ion-induced amorphous columns) increases the high-field J_c and extends the irreversibility region.

These features are all consistent with a model in which the random probability for adjacent colony orientations leads to a large variability of J_c among different samples. In addition, the intercolony percolative paths of strongly linked material lead to bulk-like, but scaled-down, transport properties rather than those characterized by weak-linked conduction. This view indicates that percolative current path options are greater for a conductor that is much larger (i.e., wider) than the typical colony size.

To test this hypothesis, measurements were conducted on the same samples as they were sequentially and progressively patterned to narrower bridge widths. The sequences of widths used were 8 mm (the full width of the sample deposited on polycrystalline yttria-stabilized zirconia), 4 mm, 1 mm, and 100 μm. The findings on one sample are shown in Fig. 1.10 where the apparent J_c is plotted (1) as a function of sample widths down to ~ 1 mm and (2) for three other samples from the same batch that had been patterned to 100-μm-wide bridges. As expected, current conduction is most effective for the full sample width where the material carried a current of 17 A in self field, corresponding to an apparent J_c = 70,000 A/cm^2. A substantial falloff in J_c occurs for a film width <4 mm; an apparent rapid decline occurs as the bridge width is decreased below the average colony size. Additional support for this model arises from the fact that nearly the same relative effect of sample width is observed both in self field and at 1 T, which is consistent with a reduced

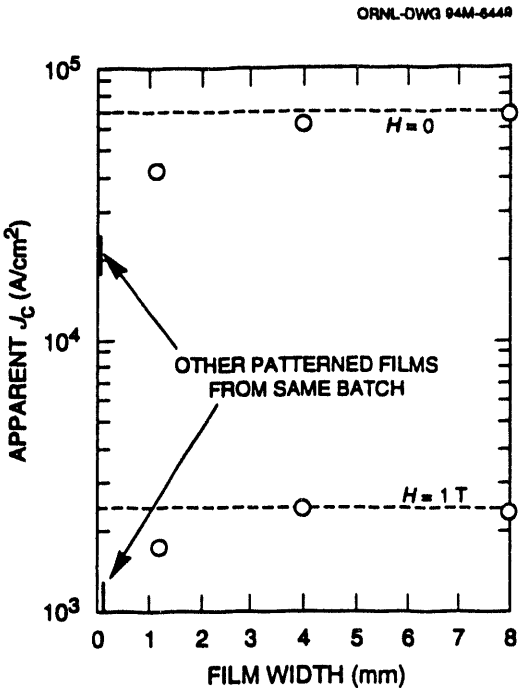

Fig. 1.10. The *apparent* critical current density of a Tl-1223 deposit as a function of the sample width as the same sample was progressively patterned to narrower conductance bridge widths. The measurements were done at 77 K; results are shown in self field and for an applied magnetic field of 1 T. The vertical bars represent the range of values measured on three other samples from the same batch that were patterned to 100-μm-wide bridges.

fraction of strongly linked, low-angle percolative paths at the intercolony boundaries.

Discussion and Conclusion

Results of X-ray diffraction azimuthal scans using small beams and EBSP determinations of the orientations of individual grains indicate the presence of colonies of grains with similar basal plane orientations. Colony dimensions in the plane appear to be in the range of 0.1 to 1 mm. Colonies have irregular shapes and therefore large areas of intersection. Note that these colonies are different from those in BSCCO, which consist of stacks of *c*-axis-aligned grains that are connected by twist boundaries. In these Tl-1223 deposits colony intersections are made up of a large number of *c*-axis tilt grain boundaries. Within a colony most grain boundaries have small misorientation angles and thus should not be weak links. We have proposed that long-range current transfer occurs through a percolative network of small-angle grain boundaries at colony intersections.[5] The number of such small-angle grain boundaries should increase with the spread in orientation of grains within a colony and with any tendency for adjacent colonies to have similar orientations such as those that might result from a local bias of colony orientation. If colonies are randomly oriented and if each colony intersects several other colonies, a significant fraction of intersection area will likely have overlapping grain orientation distributions.

Strongly linked current flow in BSCCO powder-in-tube (PIT) conductors has been discussed primarily in relation to the "brick wall" model for conduction in *c*-axis-aligned materials.[6-8] Conduction in the *c* direction through *c*-axis twist grain boundaries is an essential element of that model. It is believed, on the basis of the published results,[9,10] that *c*-axis tilt grain boundaries with large misorientation angles ($\geq 10°$) are weak links. In an idealized brick wall model of the microstructure of a *c*-axis-aligned material, current may avoid these weak links by flowing through *c*-axis twist boundaries, which may also be Josephson junction limited; but grains with large-aspect ratios have much larger areas. Studies have shown that J_c improves in Bi-2223 powder-in-tube conductor as the number of Bi-2212 intergrowths decreases at *c*-axis twist boundaries.[11] This evidence supports the importance of *c*-axis conduction in that material. On the other hand, others have found that the temperature dependence of J_c in Bi-2223 tapes is inconsistent with *c*-axis conduction and have proposed that current

flows through complex boundaries (with both twist and tilt components) that have relatively small *c*-axis misalignment and occur frequently in the imperfectly *c*-axis-aligned PIT materials.[12] We have presented a model of long-range conduction in Tl-1223 deposits in which the above controversy does not arise, since current flows through a percolative network of small-angle *c*-axis tilt boundaries, and *c*-axis conduction is not necessary. Although the relevance of these results to the more complicated microstructures in BSCCO conductors remains to be determined, it is clear that there are alternatives to the brick wall model of the microstructure that permit conduction through small-angle grain boundaries and that macroscopic determinations of texture are not adequate for delineating such structures.

Y-Ba-Cu-O Wires with Reduced Weak-Link Behavior

Microstructures in Y-124 Tapes Prepared by the Oxidation-of-Metallic-Precursor Process at American Superconductor Corporation

Multifilamentary conductors containing up to 962,000 filaments of $YBa_2Cu_4O_8$ in a silver matrix have been prepared at American Superconductor Corporation by their oxidation-of-metallic-precursor (OMP) process.[13] These materials, especially those containing the largest number of filaments, exhibit much better J_c vs H behavior than other bulk polycrystalline Y-124 and Y-123 materials. Figure 1.11 shows J_c vs H for two materials with different filament thickness. Note that the better material (containing 962,000 filaments) has a zero-field J_c = 70,000 A/cm^2, which decreases by less than a factor of 3 in a field of 0.1 T. This result indicates that weak-link behavior is very substantially reduced in this material compared with all other polycrystalline Y-124 and Y-123. The focus of ORNL's effort on these materials is to determine what aspect of the microstructure leads to strongly linked current flow.

Previous work at ORNL on grain-boundary chemistry and weak-link behavior in Y-124 provided a basis for evaluating the OMP conductor.[14] Data on magnetic susceptibility and grain-boundary chemistry were obtained on dense $YBa_2Cu_4O_8$ (Y-124) samples. TEM showed that the grain boundaries were free of second phases and that the dislocation density was low. Cation content, oxygen composition, and hole density were determined by the combined techniques of nanoprobe energy-dispersive X-ray spectroscopy and electron-energy-loss spectroscopy. Twenty-five pairs of grains were analyzed, the results of which indicated that grain boundary and bulk compositions do not differ. The relative orientations of the crystallites were determined, and the results showed that a wide variety of misorientations was sampled. Almost all of the grain boundaries were fully oxygenated (and no hole deficiencies were evident), but the magnetic-susceptibility measurements showed that the material is granular. Y-124 is thus a material in which clean, stoichiometric boundaries form weak links.

As expected, TEM examinations of grain boundaries in the OMP conductor determined that they were similar to those in sintered specimens (i.e., they were stoichiometric with respect to both cations and oxygen and showed no evidence of hole deficiency). The Y-124 grain size was also found to be very small (i.e., less than 1 μ parallel to the basal plane and $\sim$0.1 μm thick. Convergent beam electron diffraction patterns indicate that (1) locally the *c*-axis alignment is much better than indicated by macroscopic X-ray diffraction measurements and (2) locally the *a* axes of grains tend to differ in direction by less than about 15 to 20°. A general tendency for *a*,*b* axes to align parallel to the tape axis was observed, and measurements in several locations suggested the presence of colonies

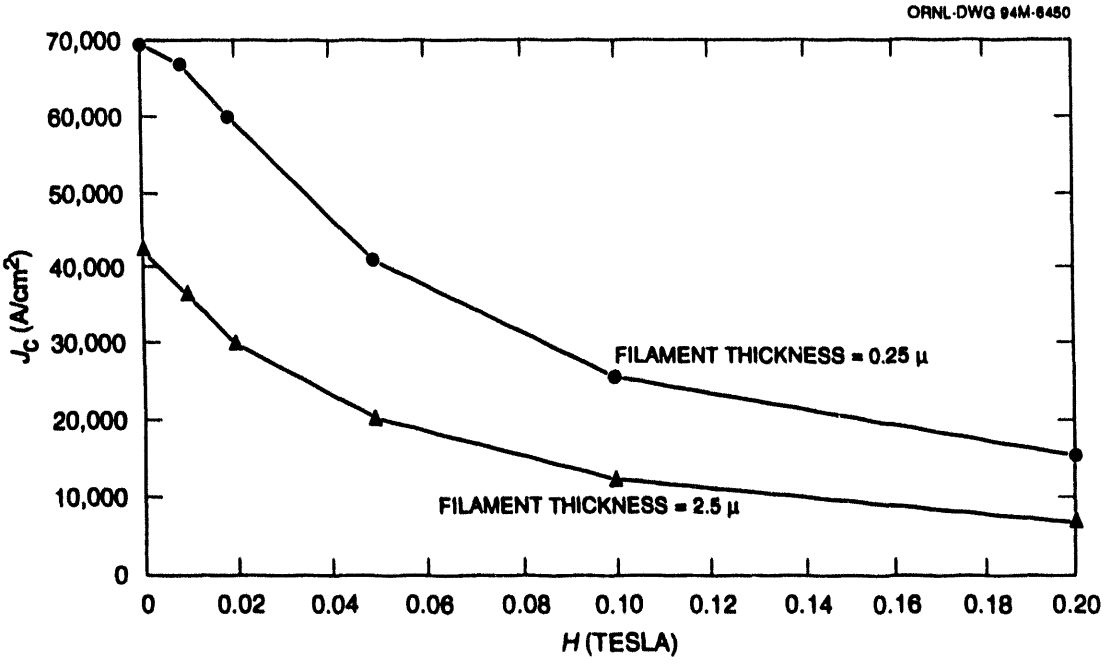

Fig. 1.11. American Superconductor's Y-124 conductor prepared by oxidation of the metallic precursor. Shown is the influence of filament size on J_c performance.

of grains with similar but not identical basal plane orientations. A determination of in-plane texture from an x-ray diffraction azimuthal scan is in general agreement with these conclusions. Further investigation of these materials using electron backscatter diffraction to obtain a map of local grain orientations is planned. We conclude that the reduction of weak-link behavior results from local in-plane texture involving colonies of grains, perhaps similar to those we have observed in General Electric Company's T-1223 deposits.

Microstructural Characteristics and Superconducting Properties of Superplastically Deformed Y-123–Silver Composites

This project was conducted in collaboration with Russell Chou of Lehigh University who, together with his student, developed process parameters for superplastic deformation of Y-123. At ORNL superconducting properties and microstructure were determined at stages in a sequence of heat treatments of deformed material. This project is part of a continuing effort to study the effects of novel processes on weak-link behavior and flux pinning in Y-123.

A sample containing 25 vol % silver–75 vol % Y-123 was compressed to over 110% at 850°C in air. Measurement of the strain rate sensitivity at 850°C yielded a value of ~0.57. This value lies in the range of 0.3 to 1.0 for most superplastic materials. The strain rate sensitivity is close to that predicted by the grain boundary sliding model for superplastic behavior; hence, grain-boundary sliding is considered to be the dominant deformation mechanism. The deformation experiments were carried out at Lehigh.

SEM examination of the as-deformed and an undeformed control sample indicated that, after deformation, significant *c*-axis texture is produced parallel to the pressing

direction. The morphology of the silver phase within the deformed sample appears to vary as a function of position or local stress; smaller size and higher aspect ratio are near the center. However, no preferential orientation of silver was observed. TEM examination showed no silver coating on Y-123 grain boundaries in the as-deformed sample, which indicated that the deformation behavior was characteristic of Y-123. All grain boundaries examined were clean in the sense that no secondary phases were present. Magnetic susceptibility measurements on the as-deformed sample indicated a T_c onset of ~ 50 K and a transition width of ~ 40 K. TEM examination also showed that all grains in the deformed sample were highly defected and that a very high density of stacking faults was present. While grain boundary sliding is likely to be the dominant deformation mechanism, the high density of defects within the grains suggests some contribution from intragranular mechanisms.

Because the deformed sample had a high density of defects and because the grain boundaries were particularly clean and sharp, the potential exists for such materials to exhibit unique superconducting properties under conditions of optimal defect densities and oxygen concentration. To explore this possibility, low-temperature heat treatments in oxygen were conducted to "fully oxygenate" the sample. This raised the T_c onset to ~ 70 K and the T_c width to ~ 30 K. Subsequent low-temperature heat treatments were unsuccessful in raising T_c. The T_c appeared to have stabilized at ~ 70 K. The possibility exists that this may have been caused by low-energy defect configurations within the grains.

To anneal out some defects and/or to modify the existing defect distribution, several successive high-temperature treatments were conducted. Heat-treatment temperatures were chosen to ensure that no bulk melting of either the silver or Y-123 occurred. The annealing time at high temperature was kept low (2 h) to minimize possible grain growth. The T_c was monitored as a function of the heat treatment. These heat treatments were successful in raising the T_c onset to ~ 90 K. However, the transition was still quite broad (i.e., a width of ~ 30 K). From this point on, magnetization data as a function of temperature and field was acquired as a function of successive heat treatments. The J_c was calculated from magnetization hysteresis using Bean's critical state model. Assuming that the size of the circulating loop equaled the sample dimensions, a value of $\sim 10^5$ A/cm^2 was obtained at 5 K and zero field and a value of $\sim 3 \times 10^4$ A/cm^2 at 5 K and 2 T (the field was applied perpendicular to the pressing direction). Further high- temperature treatments resulted in sharper transitions ($\sim$20-K width); a slight increase occurred in J_c. This was followed by extended low-temperature oxygen anneals to further sharpen the transition. Initial, low-temperature oxygenation had no effect on the transition, and further treatment resulted in a "step," or "knee," in the magnetic susceptibility at ~ 84 K; no significant change was evident in the transition width, and little effect was noted on J_c.

Next, a smaller piece was cut from the original sample to determine if any anisotropy was present in the sample for applied fields parallel or perpendicular to the pressing direction. Table 1.1 shows the results obtained using the entire sample dimensions to calculate the J_c.

These J_c values and the anisotropy in J_c for fields parallel and perpendicular to the pressing direction are similar to that obtained for melt-processed Y-123.

Because high J_c's were obtained assuming the sample dimensions as the size of the circulating loop, we intensified our study of intergrain properties. Direct current magnetic susceptibility studies were conducted to establish the nature of intergrain connectivity. Zero-field cool measurements in small magnetizing fields in the range of 0 to 20 G indicated the presence

Table 1.1. Heat treatment results on a superplastically deformed 75% Y-123–25% silver sample

Temperature	Field (T)	J_c (parallel) (A/cm^2)	J_c (perp.) (A/cm^2)	J_c (perp.)/J_c (para.)
5 K	0	8×10^5	2×10^5	4
	2	2×10^5	7×10^4	2.8
20 K	0	3×10^5	9×10^4	3.3
	2	5×10^4	1×10^4	5
60 K	0	5×10^4	1.5×10^4	3.3
	2	3×10^3	1×10^3	3

of steps, or knees, that had strong dependence on the applied magnetic field. Increasing applied fields caused the position of the knee to move rapidly downward in temperature. This behavior is a characteristic signature of "weak links" or poor intergrain connectivity. However, because extremely high J_c values are obtained using sample dimensions, it is not clear if the weak-link behavior observed at relatively high temperatures is retained at lower temperatures. Because the Josephson current is not expected to be too strongly temperature dependent, retention of weak-link behavior to low temperatures is likely.

Optical microscopy indicated that, after the final heat treatment, significant grain growth had occurred. The average grain size was estimated to be ~ 30 μm (compared with ~ 1 μm starting grain size). By assuming this grain size for calculation of J_c, values higher by a factor of 30 than those listed above are obtained. The microstructure of the annealed sample indicated that a large portion of the apparent deformation-induced texture was lost during recrystallization and grain growth. The measured J_c values likely may be explained by a combination of increased intergranular J_c, as well as the presence of some strongly coupled grain boundaries, yielding effective current loops larger than the average grain size. Future TEM examination of the sample in its present state would reveal the nature, density, and distribution of pinning centers within the grains.

In summary, heat treatments were carried out on a superplastically deformed 75% Y-123–25% silver sample with the aim of optimizing superconducting properties. Results indicate the presence of unusually high critical currents at low temperatures. These observations may be explained by highly superior intragranular properties coupled with increased local loop size (i.e., the fraction of neighboring grains that are strongly linked is increased).

Tl-1233 POWDER-IN-TUBE CONDUCTOR FABRICATION AND PROCESSING

The processing of PIT conductors containing aerosol, flow reactor–produced powders has been studied. Aerosol powders have been prepared both with thallium in the flow reactor system and as thallium-free precursors to which thallium is added in a subsequent process. PIT conductor has been fabricated and processed using aerosol powders with the compositions $Tl_{0.5}Pb_{0.5}Sr_{2.0}Ca_{2.0}Cu_3O_x$, $Tl_{1.2}Ba_{2.0}Ca_{1.9}Cu_3Ag_{0.8}O_x$ and $Tl_{0.8}Ba_{1.9}Ca_{2.0}Cu_3Ag_{0.35}O_x$. Conductor containing the last composition, prepared as a thallium-free precursor, has been extensively studied, since this composition matches that of General Electric Company's high-J_c spray-pyrolyzed deposits. Note that for this composition containing barium without strontium, only aerosol powders have been found by Intermagnetics General Corporation to convert to the Tl-1223 phase in PIT form. Typical morphology of the powders is shown in Fig. 1.12.

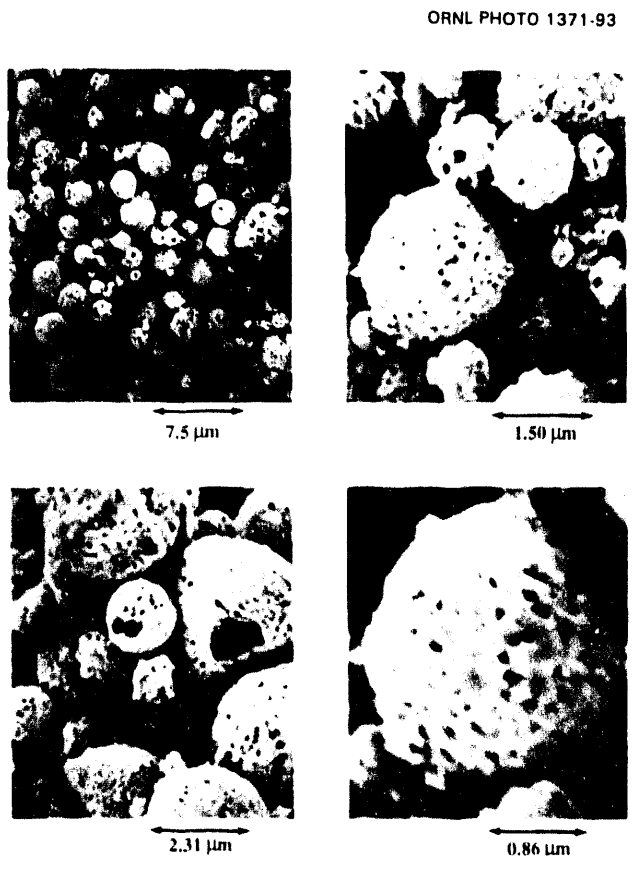

Fig. 1.12. Typical morphology of aerosol powders that convert to the Tl-1223 phase in powder-in-tube form.

Subsequent to aerosol synthesis, the thallium-free precursor was vacuum-treated at 700°C to remove any residual nitrates. The powders were then mechanically mixed with appropriate amounts of Tl_2O_3 and heat-treated at ~650°C in a sealed capsule. The purpose of this heat treatment was to decompose Tl_2O_3, resulting in the formation of Tl_2O vapor. It was hoped that a more homogeneous distribution of thallium would be achieved on cooling than that attained by mechanical mixing. SEM examination of the thallinated powders indicated that each individual particle ~1 to 2 μm in size was composed largely of thin plate-like phases and submicron ellipsoidal and rod-like phases. Energy dispersive spectroscopy analysis in SEM indicated that the plate-like phases correspond primarily to Tl-1212, while the rod-like and ellipsoidal phases correspond to nonthallium phases (e.g., BaCuO and $CaCuO_2$).

These powders were sent to Pradeep Haldar (IGC) for fabrication into a PIT tape. Figure 1.13 shows a differential thermal analysis and thermogravimetrical analysis trace (in air) of a PIT Tl-1223 sample. Onset of melting was close to 830°C, and a characteristic two-step melting behavior was noted such as that observed with all compositions studied so far. Heat treatments were designed to probe the effect of melt-processing at temperatures near and within the endotherm. A typical processing schedule is indicated in Fig. 1.14. Sharp transitions were obtained under a variety of heat-treatment conditions (summarized in Tables 1.2 through 1.4). A typical resistive transition is shown in Fig. 1.15. All samples were characterized with respect to their J_c's at 77 K in fields up to 1 T. Figure 1.16 shows a typical variation of the critical current density at 77 K. Zero-field J_c's range from 1 to 8 × 10^3 A/cm^2. All tapes processed thus far are characteristically weak-linked (over a hundred samples have been tested) but have a plateau extending to high fields. Compared with the best published data on Tl-1223 PIT,[15] these samples are more severely weak-linked and have lower zero-field J_c (by a factor of 3).

Figure 1.17 shows the morphology of peeled tapes. The cracks seen in the low-magnification micrograph are perhaps

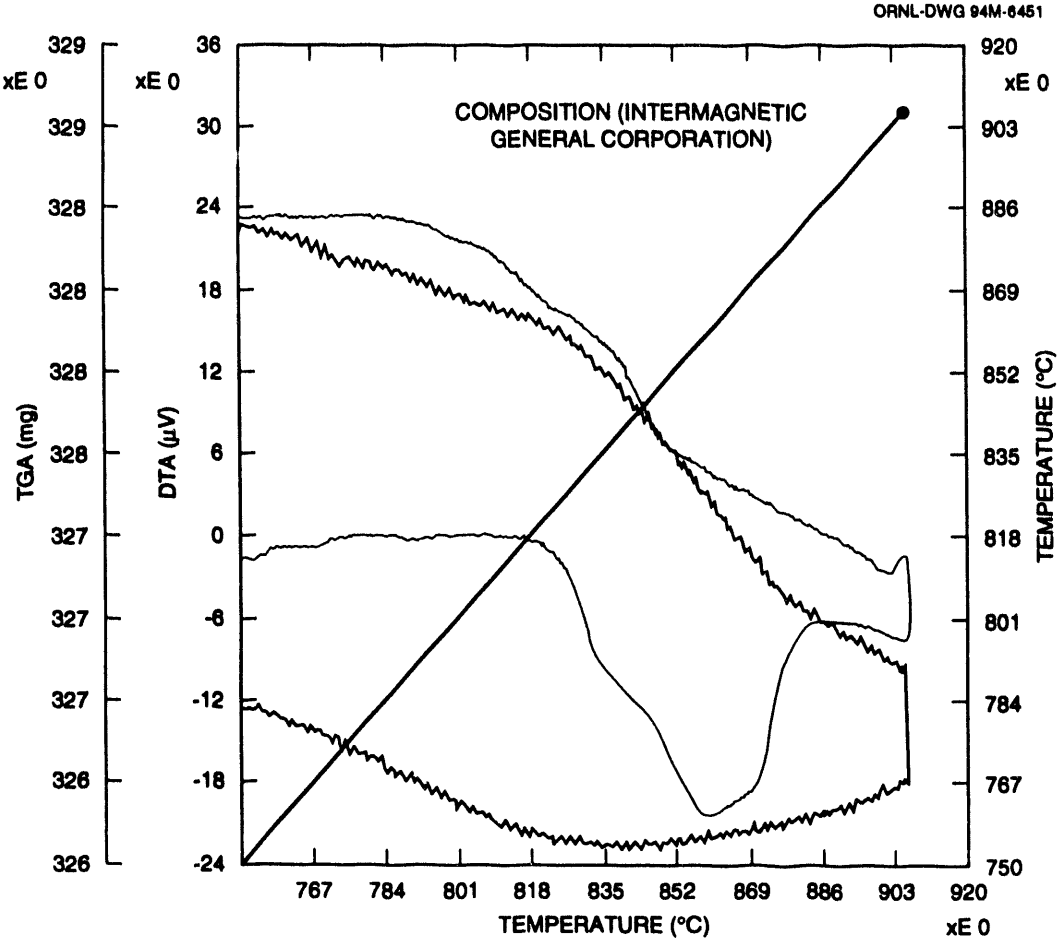

Fig. 1.13. Thermal analysis of power-in-tube $Tl_{0.8}Ba_{1.9}Ca_{2.0}Cu_{3.0}Ag_{0.35}O_x$. DTA—differential thermal analysis; TGA—thermogravimetrical analysis.

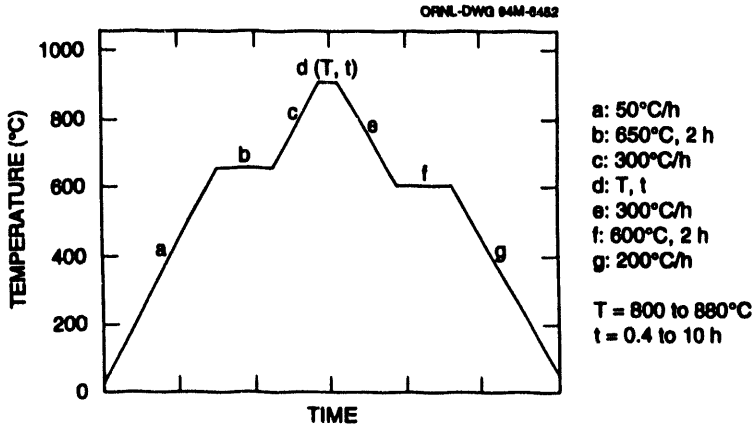

Fig. 1.14. Typical processing schedule for aerosol powders.

produced by the fracturing process. Large amounts of porosities, which are largely a consequence of the random texture of the plate-like Tl-1223 platelets, are produced. Also present are significant quantities of secondary-phase particles, many of which correspond to $CaCuO_2$.

The effect of short heat-treatment times as a function of the peak processing temperature on the properties is indicated

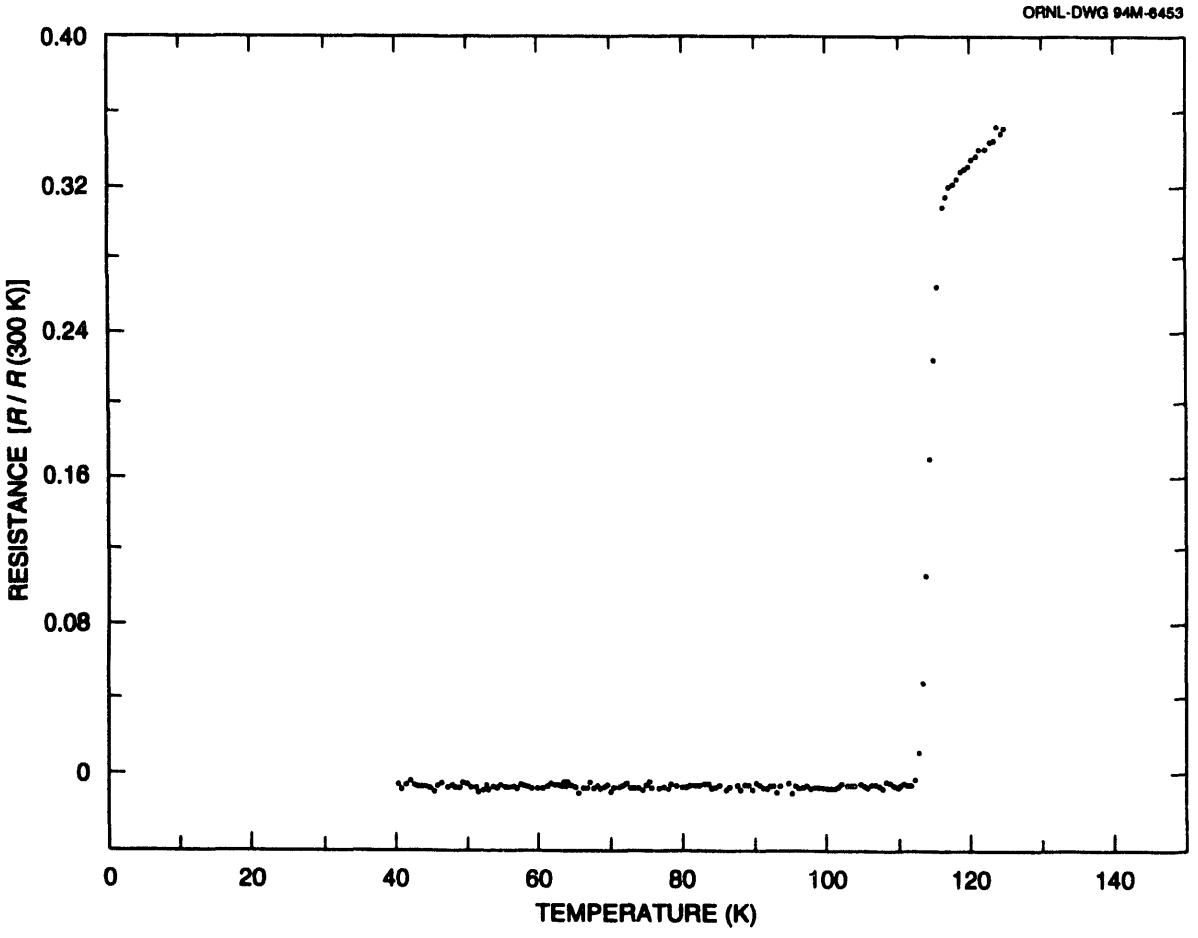

Fig. 1.15. Typical resistive transition.

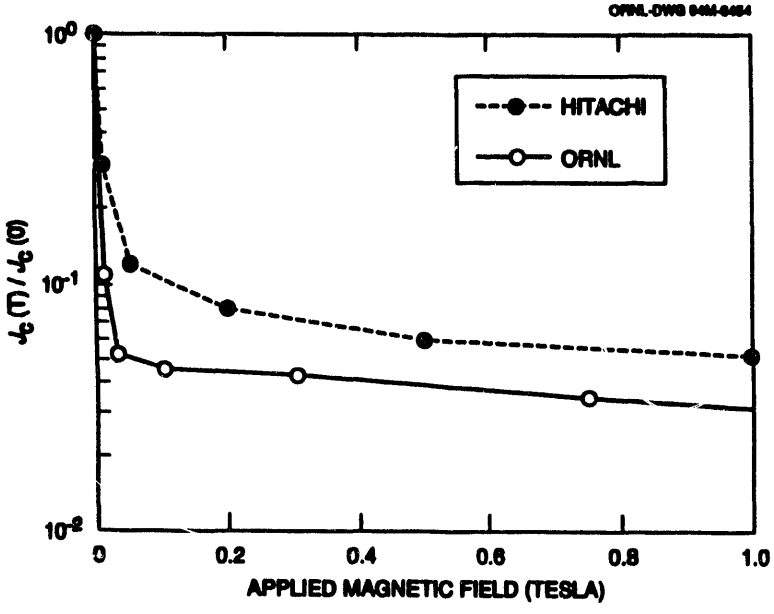

Fig. 1.16. Typical variation of the critical current density at 77 K. Tapes are weak-linked but have a plateau extending to high fields.

in Table 1.2. The dashes in all tables indicate that the particular measurement was not made. The highest zero-field J_c's are obtained for treatments at 830°C. However, the drop in J_c is less severe for samples processed at higher temperatures. The critical current at zero field is plotted as a function of sintering temperature in Fig. 1.18, showing the presence of a relatively narrow window for processing.

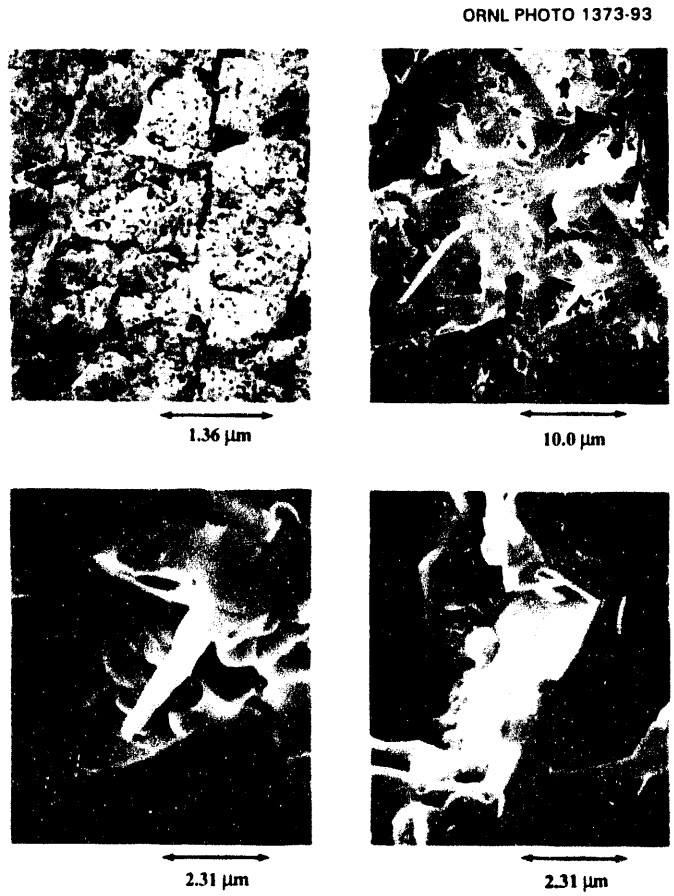

Fig. 1.17. Morphology of peeled tapes.

Comparing this data with the differential thermal analysis trace, it appears that higher J_c is obtained when a small amount of liquid is present. Note that no transition was observed for the sample processed at 810°C, suggesting that incipient melting may be necessary to form the Tl-1223 phase.

The effect of heat-treatment time at the optimum temperature is shown in Table 1.3. Heat treatments of 2 h yielded the highest critical currents. Although not indicated in the table, sintering times as low as 15 min were tried. Results showed that J_c increases with time until ~2 h, again implying some parabolic dependence. The effect of longer heat treatments as a function of temperature are indicated in Table 1.4. Increasing

Table 1.2. Effect of heat treatment temperature (short heat treatments)

Sample	Temp. (°C)	Time (h)	T_c onset (K)	T_c zero (K)	I_c (0 T) (A)	I_c (0.01 T) (A)	I_c (1 T) (A)	I_c (0 T)/ I_c (0.01 T)	I_c (0 T)/ I_c (1 T)
2517-20	810	2 h	0	0	-	-	-	-	-
2505-7AG (2505)	820	2 h	111	107	3.6	0.18	0.09	20	40
2478-2481AG (2480)	830	2 h		-	5.6	0.78	0.14	7.2	40
2512-15AG (2486)	840	2 h	113	111	4.1	0.5	0.15	8.2	27
2485-2488AG (2486)	850	2 h		-	2.83	0.37	0.08	7.7	36
2491-94AG (2491AG)	860	2 h		-	0.17	0	0	0	0

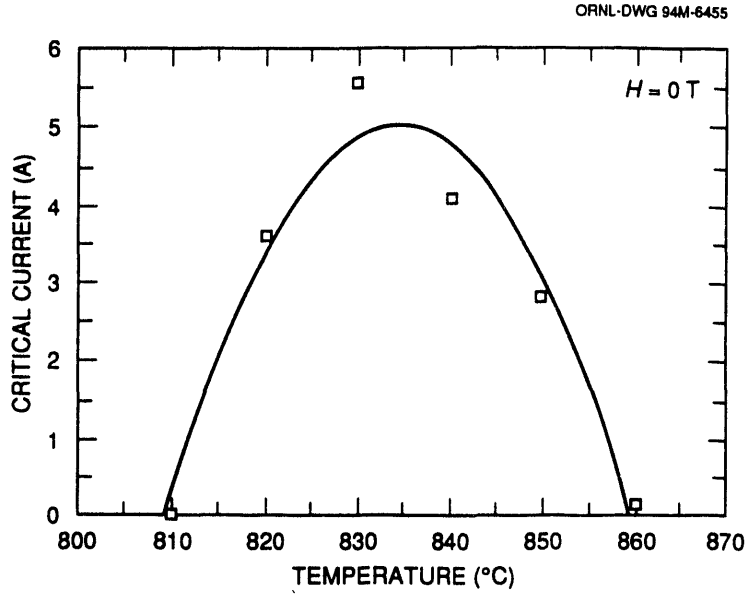

Fig. 1.18. Critical current at zero-field plotted as a function of sintering temperature.

the sintering time from 2 to 10 h resulted in an onset T_c at 810°C. The transition was, however, not complete. As is indicated in the table, for a sintering time of 10 h, the maximum J_c was obtained for a sintering temperature of 830°C. For temperatures above 840°C, thallium loss is perhaps too severe. Table 1.4 shows properties of tapes sintered for 24 h. In this case relatively sharp transitions were also obtained for samples sintered as low as 800°C. The highest J_c was obtained for a sintering temperature of 810°C. These longer heat-treatment time samples were produced to see how the J_c's of "sintered" samples compared with "melt-sintered" samples.

In looking at the overall data, we found that samples with higher zero-field J_c's had larger drops in J_c in fields up to 1 T. This may suggest that higher J_c samples contain a larger fraction of links that are "weak" as opposed to a larger fraction of strongly linked grain-boundary area. Some lower J_c samples exhibit a small peak effect (Fig. 1.19).

The effect of postoxygenation at 600°C was also investigated. The effect of oxygenation was very small—showing slight increases in the zero-field J_c. The effect of uniaxial pressing and the number of pressings/sinterings on these samples will be published in a separate document.

BSCCO POWDER-IN-TUBE AND DEPOSITED CONDUCTOR DEVELOPMENT

Powder-in-Tube

PIT conductor development work is being conducted in cooperation with American Superconductor Corporation (ASC) through the Wire Development Group. Activities include (1) development of aerosol pyrolysis technology for preparation of highly homogeneous Bi-2223 powders, (2) studies of the effects of fabrication variables on dimensional stability of the core and the quality of the silver/superconductor interface, and (3) determinations of the mechanical properties (microhardness and modulus) of superconducting and secondary phases using the Nanoindenter facility in the High-Temperature Materials Laboratory.

Aerosol Pyrolysis Process Development

Powders prepared by aerosol pyrolysis have very desirable characteristics for preparation of PIT conductors. Foremost is their homogeneity: each particle contains the same cations that were present in its parent aerosol droplet (in the absence of vapor losses). Furthermore, particles are small, ~1 μm, and second-phase agglomerates do not form. These characteristics are especially desirable for the fabrication of multifilamentary conductor in which filament dimensions may be comparable to the size of

Table 1.3. Effect of heat-treatment time at optimum temperature

Sample	Temp. (°C)	Time (h)	T_c onset (K)	T_c zero (K)	I_c (0 T) (A)	I_c (0.01 T) (A)	I_c (1 T) (A)	I_c (0 T)/ I_c (0.01 T)	I_c (0 T)/ I_c (1 T)
2480AG	830	2	-	-	5.6	0.78	0.14	7.18	40
2413AG	830	10	108	104	4.45	0.48	0.09	9.3	49
	830	20	-	-	-	-	-	-	-
2447AG	830	30	117	105	3.54	0.276	0.1	12.8	35.4
	830	40	-	-	-	-	-	-	-
	830	50	-	-	-	-	-	-	-

Table 1.4. Effect of heat treatment temperature (long heat treatments)

Sample	Temp. (°C)	Time (h)	T_c onset (K)	T_c zero (K)	I_c (0 T) (A)	I_c (0.01 T) (A)	I_c (1 T) (A)	I_c (0 T)/ I_c (0.01 T)	I_c (0 T)/ I_c (1 T)
2795AG	780	10	-	-	-	-	-	-	-
2785AG	790	10	-	-	-	-	-	-	-
2778AG	800	10	-	-	-	-	-	-	-
2776AG	810	10	112	-	-	-	-	-	-
2430AG	820	10	114	110	4.2	0.45	0.12	9.3	35
2413AG	830	10	108	104	4.45	0.48	0.09	9.3	49
2411AG	840	10	114	113	2.97	0.15	0.09	19.8	33
2369AG	850	10	116	80	-	-	-	-	-
2370AG	880	10	105	70	-	-	-	-	-
2795AG	780	24	108	80	-	-	-	-	-
2785AG	790	24	116	98	0.56	0.06	0.02	9.3	28
2778AG	800	24	115	106	2.44	0.13	0.05	7.4	49
2776AG	810	24	114	107	4.34	0.61	0.13	7.1	33

particles and agglomerates in powders prepared by some methods. For these and other reasons, ORNL and American Superconductor Corporation are cooperating in the development of aerosol process technology and the processing of PIT conductor containing aerosol powders. At ORNL aerosol process technology is emphasized in studies of the effects of aerosol process parameters on powder characteristics. ASC is scaling up the aerosol process for high-powder production rates and is fabricating and processing PIT conductor containing aerosol powders.

A new aerosol system with a four-zone furnace and improved control of carrier gas

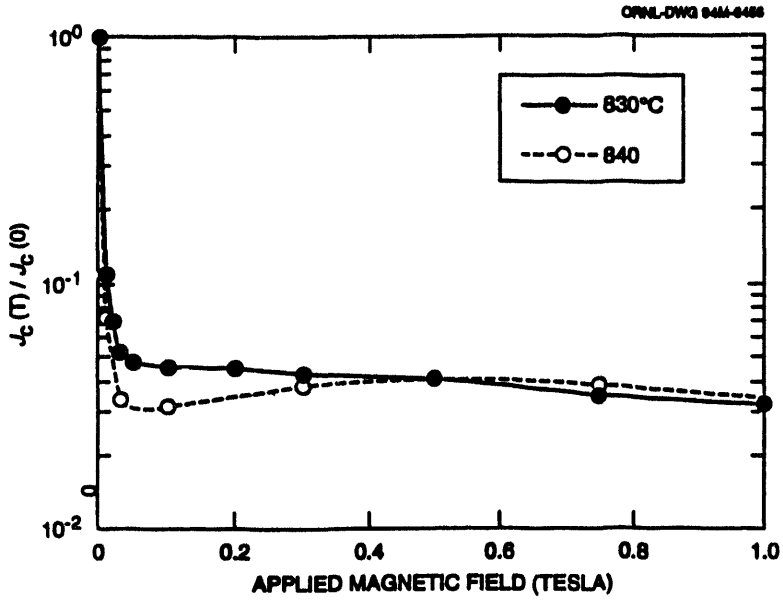

Fig. 1.19. Lower J_c samples reflecting a small peak effect.

flow rate and pressure has been constructed. Figure 1.20 shows schematically the aerosol pyrolysis system. An aerosol is generated by ultrasonic agitation of the surface of a nitrate solution containing the cations of the superconductor in the desired concentration ratio. The aerosol droplets are entrained in a carrier gas and transported through the hot zone of a furnace where drying and nitrate decomposition occurs. The resulting mixed oxide powder particles are collected on a filter. The cation ratio in each particle is the same as that of its parent solution droplet provided no components are volatilized. In the Bi-Pb-Sr-Ca-Cu-O system, PbO vapor pressures can be significant during aerosol pyrolysis. The effects of aerosol pyrolysis process parameters on lead loss have been studied extensively. Process conditions can be found that effectively eliminate lead loss. Alternatively, if a desired phase assemblage cannot be obtained without lead loss, it is possible to compensate accurately for lead loss by adjusting the lead concentration in the nitrate solution.

The effects of pyrolysis temperature particle residence time in the hot zone, and oxygen partial pressure in the carrier gas on phase assemblage and particle morphology, have been preliminarily investigated. The effect of pyrolysis temperature on phase assemblage and lead loss at one oxygen partial pressure, 5% O_2, has been determined, as has the effect of oxygen partial pressure at one temperature, 800°C. In both cases, a wide range of phase assemblages was obtained. Particle morphologies range from hollow spheres at low pyrolysis temperatures to dense faceted particles at high temperatures. The results clearly demonstrate that lead loss can be controlled and that a range of phase assemblages can be prepared.

Aerosol powder must be given a postsynthesis heat treatment to remove residual nitrates and CO_2 that are present in as-synthesized powder owing to "back-reaction" with NO_x and contaminants in the carrier gas stream while the particles are on the collector. The effect of oxygen partial and treatment temperature on the CO_2 and NO_x content and phase assemblage of treated powders has been studied. Under optimal conditions powders with virtually undetectable carbon concentrations (<50 wt ppm) can be prepared.

Over the past year ASC has fabricated several PIT tapes containing aerosol powders prepared at ORNL with characteristics specified by ASC. Critical current densities have steadily improved to ~15,000 A/cm^2 at 77 K, $H = 0$.

Deformation Processing Studies

In cooperation with ASC, the effects of conductor fabrication variables on dimensional stability of the core and the

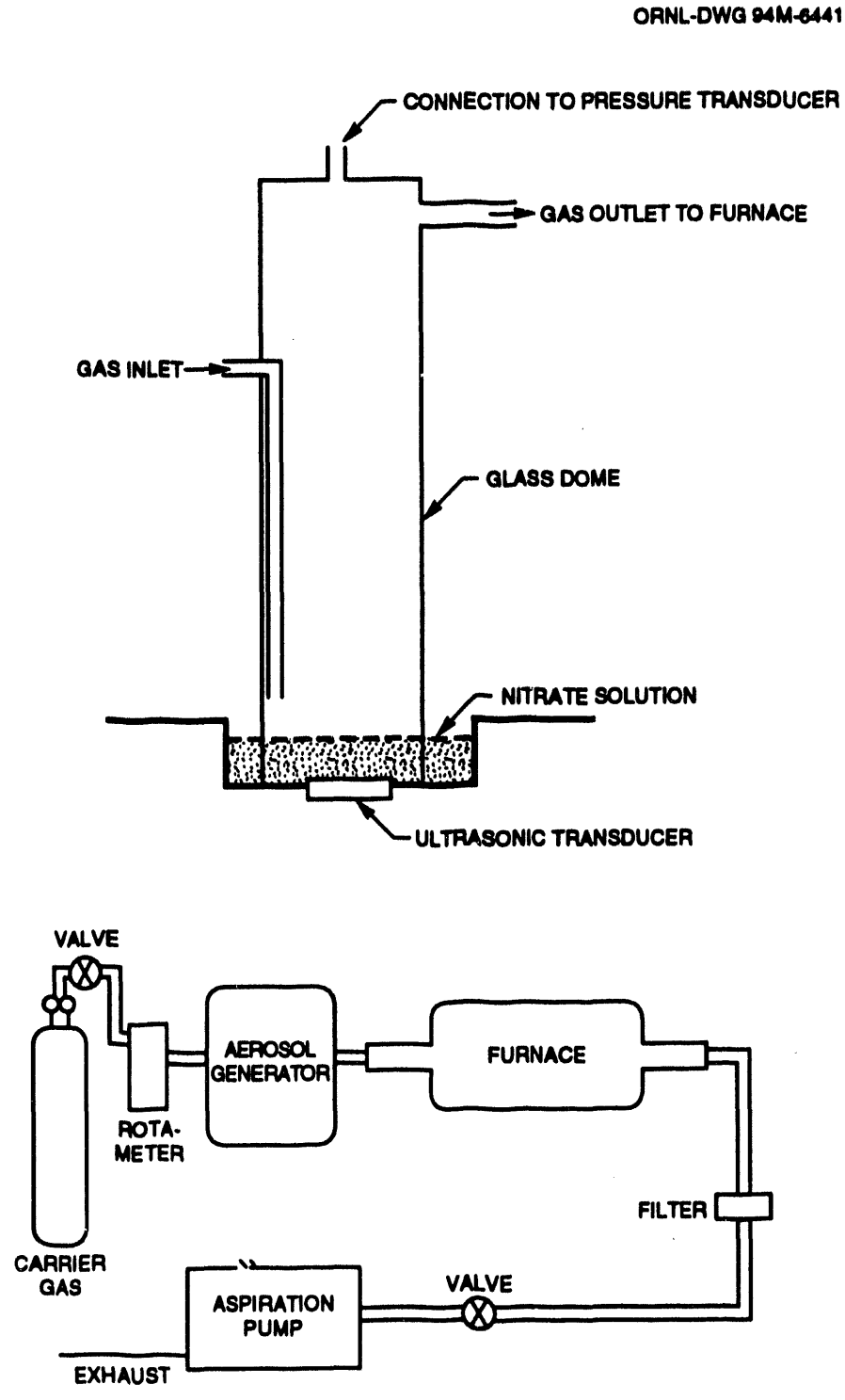

Fig. 1.20. Aerosol pyrolysis system. Advantage: powders have small particle size, no hard agglomorates, and excellent homogeneity as needed for multifilamentary conductor with very small filaments. Key process parameters: pyrolysis temperature, residence time, and carrier gas composition, P (O_2).

smoothness of the superconductor-silver interface have been studied. Investigation of the initial fabrication prior to the first heat treatment has been emphasized, and the effects of such variables as rolling speed and reduction/pass have been investigated. Results of this work are presented on a limited access basis at the Wire Development Group meetings.

Mechanical Properties of Superconducting and Secondary Phases in Bi(Pb)-2223 Powder-in-Tube Conductor

This project is being conducted in cooperation with American Superconductor Corporation using the Nanoindenter facility in ORNL's High-Temperature Materials Laboratory through a nonproprietary user agreement.

One objective of the project was to determine the elastic modulus and hardness of various phases encountered in BSCCO PIT conductors. Mechanical property data are required as input parameters in a numerical simulation of oxide PIT processing. No good elastic data exist for BSCCO Bi-2212 and Bi-2223 phases. Furthermore, no direct measurements have been made on PIT materials, the microstructure and compositions of which are unique.

Experiments were performed using the Nanoindenter (trademark of Nano Instruments, Inc.), a highly spatially resolved mechanical properties microprobe. The mechanical properties were determined by moving the Nanoindenter into the surface of the specimen with a precisely controlled load while continuously monitoring the vertical displacement associated with the indentation process. The Nanoindenter used was a Berkovich, three-sided, triangular-shaped diamond pyramid. It has the same area-to-depth function as a Vickers pyramid. The specimens were rigidly mounted on a motorized *xy* table having a resolution of ± 1 μm. The vertical displacement of the Nanoindenter was monitored by a capacitive displacement gage with a resolution of ~ 0.5 nm. The load on the Nanoindenter, generated using a calibrated coil and magnet by varying the current through the coil assembly, offered a force resolution of ~ 0.5 mN. Figure 1.21 shows a schematic representation of a typical load-displacement curve consisting of a single loading cycle. The inset shows the cross section of the indentation process.

A single test in this study consisted of 12 steps:

- surface approach and contact,
- constant loading at 3 nm/s to a depth of ~ 100 nm,
- holding for 15 s,
- constant unloading to 80% of the maximum load,
- constant loading at 3 nm/s to a depth of ~ 200 nm,
- holding for 15 s,
- constant unloading to 80% of the maximum load,
- constant loading at 3 nm/s to a depth of ~ 300 nm,
- holding for 15 s,
- constant unloading to 80% of the maximum load,
- 100-s holding for thermal drift determination, and
- constant unloading to zero load.

A typical load-displacement curve is shown in Fig. 1.22. It was assumed that the material does not change during this loading cycle. Indenter shape calibration was done by making measurements on a standard material, fused silica. About 20 indentations were made in the same orientation for each material. Table 1.5 summarizes the results.

Deposited Conductor Development

The objective of the agreement with Westinghouse Electric Corporation is to

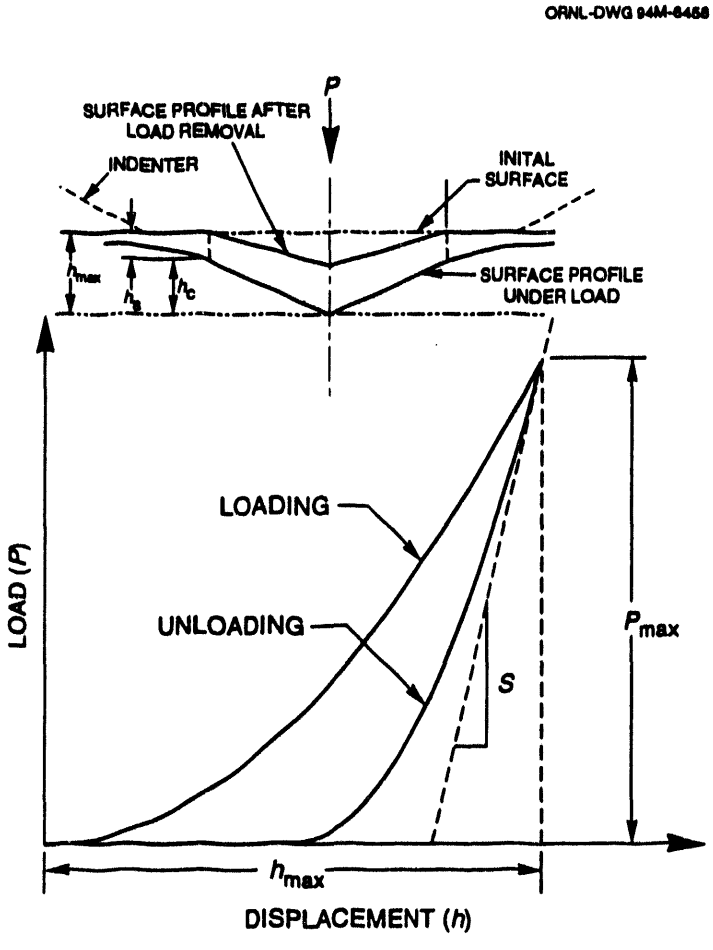

Fig. 1.21. Typical load-displacement curve consisting of a single loading cycle. Inset: cross section of the indentation process.

develop the technology to determine and to demonstrate processes needed for the fabrication of high-J_c conductors for electric power utility applications. Activities have been divided into those related to short-length lead applications and those related to long-length conductor applications.

Short-length lead activities have focussed on developing materials-processing methods [including cold isostatic pressing (CIP), hot isostatic pressing (HIP), and suction casting] for fabrication of prototypic high-current, high-temperature superconducting leads with sufficiently high-fracture toughness and elasticity. Cylindrical rods (~ 1 cm long and ~ 1 cm ϕ) with integral silver end caps have been prepared by a single CIP operation from both BSCCO Bi-2212 and precursor BSCCO Bi-2223 powders. Subsequent HIP operations performed on some of the CIP rods have been complicated by interactions of the superconducting oxides with the steel HIP containers. The CIP and CIP/HIP rods have been given a variety of thermal treatments, and the resulting materials have been characterized metallographically and by X-ray diffraction. Approaches to improve the dimensional uniformity of the leads and the integrity of the silver-oxide bond are under consideration.

Suction casting, a method in which a liquid is rapidly cast into a containment tube, has been explored as a means of fabricating short-length leads for various process conditions (e.g., temperature of the melt, casting tube material and diameter, and vacuum dynamics). Preliminary results are encouraging.

Long-length conductor activities have dealt with fabrication of silver-sheathed BSCCO Bi-2223 ribbon conductors from spray-dried aerosol powder precursors on silver strips. Efforts have been divided between processing of individual predeposited silver strips and incorporating a number of these strips into a suitable conductor geometry.

The processing of individual predeposited silver strips has been limited by slow and incomplete conversion of the precursor powder to BSCCO Bi-2223. The rate and extent of conversion has been

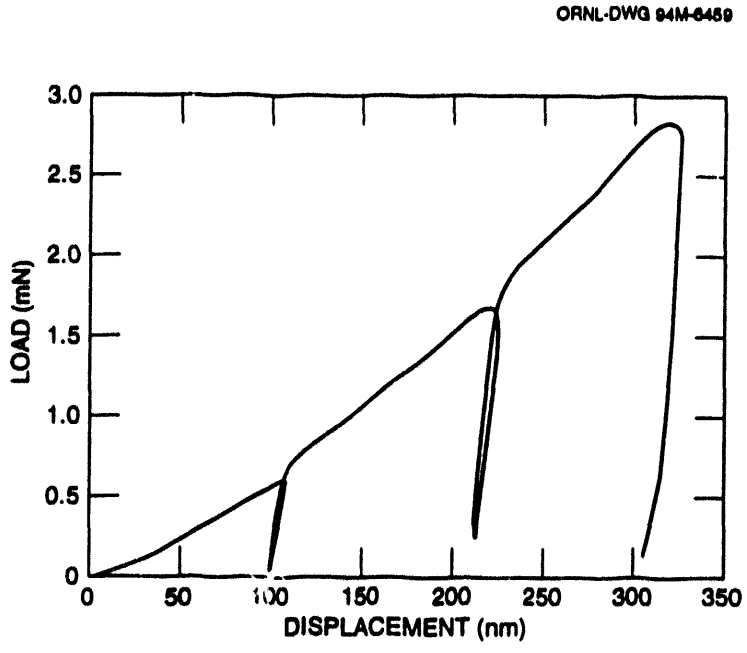

Fig. 1.22. Typical load-displacement curve.

Table 1.5. Mechanical properties of BSCCO power-in-tube samples

Material[a]	Elastic modulus (GPa)	Hardness (GPa)
Bi-2212 (100) or (010)	93.8 ± 3.5	2.3 ± 1.3
Bi-2212 (001)	49.8 ± 11.6	2.7 ± 1.2
Bi-2212 (as rolled)	64.9 ± 4.5	2.4 ± 0.4
Bi-2223 (100) or (010)	90.2 ± 9.5	1.9 ± 0.5
Bi-2223 (001)	54.4 ± 1.8	1.5 ± 0.7
Second phase	59.6 ± 6.5	2.4 ± 0.4

Material	Elastic anisotropy (100)/(001)	Hardness anisotropy (100)/(001)
Y-123[b]	1.3	0.9
Bi-2223	1.7	1.1
Bi-2212	1.9	0.9

[a]The elastic modulus of Bi-2212 and Bi-2223 is highly anisotropic. The higher compressability along the *c* direction is due to the layered structure.
[b]Compared with Y-123, the BSCCO phases are much softer and less stiff.

shown to be extremely sensitive to the properties of the aerosol powder as well as to the conditions during heat treatment. Conversion seems to depend critically on the presence or absence of a yet unidentified metastable crystalline phase in the aerosol powder. This behavior is observed for both thick deposits of powder on silver and bulk pellets of compressed powder. Efforts to identify this phase and perhaps understand its role in conversion are continuing. Statistical optimization of the conditions during heat treatment to maximize J_c has been initiated. Replication studies for selected furnace systems at both ORNL and Westinghouse Electric Corporation have been completed.

A method to fabricate silver-sheathed BSCCO Bi-2212 and Bi-2223 ribbon conductors has been investigated. This method involves stacking predeposited silver strips into a silver or silver alloy encasement. The encasement is then rolled and heat-treated to form the conductor. Studies have been undertaken to evaluate the stability of the multilayered geometry of the resulting conductor for various deformation and heat-treatment schedules. Metallographic examinations suggest that the continuity of the oxide layers degrades most severely during heat treatment (815°C, 100 h, in air). Electrical transport results are consistent with oxide discontinuity. An alternate approach to rolling (i.e.,

hydrostatic extrusion followed by drawing of a split silver insert) is being considered to reduce the problem of oxide layer instability.

References

1. J. A. DeLuca et al., "The Preparation of 1223 Tl-Ca-Ba-Cu-Oxide Superconducting Films via the Reaction of Silver-Containing Spray Deposited Ca-Ba-Cu-Oxide with Thallium Oxide Vapor," *Physica C* **205**, 21-31 (1993).
2. J. E. Tkaczyk et al., "Transport Critical Currents in Spray Pyrolyzed Films of $TlBa_2Ca_2Cu_3O_x$ on Polycrystalline Zirconia Substrates," *Appl. Phys. Lett.* **61**(5), 610-12 (1993).
3. J. E. Tkaczyk et al., "Enhanced Transport Critical Current at High Fields After Heavy Ion Irradiation of Textured $TlBa_2Ca_2Cu_3O_x$ Thick Films," *Appl. Phys. Lett.* **62**(23), 3031-33 (1993).
4. D. J. Miller et al., "Brick-Wall Structure in Polycrystalline $TlBa_2Ca_2Cu_3O_x$ Thick Films with High Critical Current," *Appl. Phys. Lett.* **63**(4), 556-58 (1993).
5. D. M. Kroeger et al., "Local Texture and Percolative Paths for Long-Range Conduction in High Critical Current Density $TlBa_2Ca_2Cu_3O_{8+x}$ Deposits," *Appl. Phys. Lett.* **64**(1), 106-108 (1994).
6. A. P. Malozemoff, "Critical Current Density of High Temperature Superconductor," in *High Temperature Superconducting Compounds II*, ed. S. H. Whang, A. DasGupta, and R. B. Laikowitz, TMS Publications, Warrendale, Pa., 1990.
7. L. N. Bulaevskii et al., "Limits to the Critical Current in High T_c Superconducting Tapes," *Phys. Rev. B* **48**(18), 13798 (Nov. 1, 1993).
8. J. Mannhart and C. C. Tsuei, "Limits of the Critical Current Density of Polycrystalline High-Temperature Superconductors Based on the Current Transport Properties of Single Grain Boundaries," *Z. Phys. B—Condensed Matter* **77**, 53-59 (1989).
9. D. Dimos et al., "Orientation Dependence of Grain-Boundary Critical Currents in $YBa_2Cu_3O_{7-\delta}$ Bicrystals," *Phys. Rev. Lett.* **61**(2), 219 (July 11, 1988).
10. D. Dimos, P. Chaudhari, and J. Mannhart, "Superconducting Transport Properties of Grain Boundaries in $YBa_2Cu_3O_7$ Bicrystals," *Phys. Rev. B* **41**(7), 4038 (1990).
11. A. Umezawa et al., "Electromagnetic Granularity, Critical Current Density, and Low-T_c Phase Formation at the Grain Boundaries in (Bi, Pb)$_2Sr_2Ca_2Cu_3O_x$ Silver-Sheathed Tapes," *Physica C* **198**, 261-72 (1992).
12. B. Hensel et al., "A Model for the Critical Current in (Bi, Pb)$_2Sr_2Ca_2Cu_3O_x$," *Physica C* **205**, 329-37 (1993).
13. L. J. Masur "Bi-axial Texture in $Ca_{0.1}Y_{0.9}Ba_2Cu_4O_8$ Composite Wires Made by Metallic Precursors," paper submitted to *Physica C*.
14. Z. L. Wang et al., "Grain-Boundary Chemistry and Weak-Link Behavior of Polycrystalline $YBa_2Cu_4O_8$," **48**(13), 9726 (Oct. 1, 1993).
15. M. Okada et al., "Weak-Link Characteristics and Transport Properties of Tl-1223 Tape-Shaped Wire," *Jpn. J. Appl. Phys.* **32**, 2634 (1993).

Technical Progress in Applications Development

DEMONSTRATION OF A MAGNETIC REFRIGERATOR FOR HIGH-TEMPERATURE SUPERCONDUCTOR DEVICE APPLICATIONS

The discovery of high-temperature superconducting materials has prompted renewed interest in applications of superconductivity. For example, superconducting magnets capable of achieving high magnetic fields have numerous existing and potential applications that include superconducting magnetic energy storage units, accelerators, motors, fusion devices, and magnetic refrigerators. Although material development efforts have raised superconducting critical temperatures substantially, eliminating the need to operate near liquid helium temperature, it appears that, for the forseeable future, practical applications will require cooling in higher portions of the cryogenic temperature range. In the near term it seems likely that temperatures below that of liquid nitrogen will be required in most practical devices. Magnetic refrigeration is a type of solid state cooling process that employs materials whose entropy characteristics can be effectively altered by magnetic fields (see Fig. 2.1). This technology offers the opportunity for improved efficiency and reliability in cryogenic cooling applications if performance estimates can be achieved in practice. A key requirement for any practical magnetic refrigeration system is the realization of relatively high magnetic fields with relatively low losses, the essentially exclusive realm of superconducting magnets (Fig. 2.2).

From the preceding discussion it is clear that superconductors need refrigeration and that magnetic refrigerators need superconductors. In other words, magnetic refrigeration represents a rare combination—both an application of, and an enabling technology for, superconductors. By the same token, the development of high-temperature superconducting materials promises reduced (but still substantial) refrigeration requirements for devices with many applications and improved refrigerators for meeting those requirements. For very large temperature lifts, such as from cryogenic temperatures to room temperature, staged refrigerators are likely to be required. The available options include not only full multistage magnetic units but also hybrid systems combining a low-temperature magnetic stage with either a closed gas cycle or open cryogen high-temperature stage. Consistent with the apparent opportunities outlined here, the objectives of this project are (1) to develop a prototypic magnetic refrigerator stage that could provide 50-W cooling at 40 K and (2) to demonstrate an integrated system using the hybrid concept.

As is indicated above, this project has a direct relationship to nearly all other projects in the U.S. Department of Energy's (DOE's) high-temperature superconductivity program in that (1) methods like that being investigated here could provide the cooling capability required to realize practical magnetic field/current density combinations with candidate high-temperature superconducting materials and (2) such materials could ultimately be employed in the magnets of the refrigerator itself.

Approach

For Task 1, Astronautics Corporation of America concentrated on design of the magnetic (lower temperature) stage of the refrigerator, including the specification of magnet and upper stage interface requirements. ORNL's Fusion Energy Division provided magnet design information to meet lower stage requirements. The

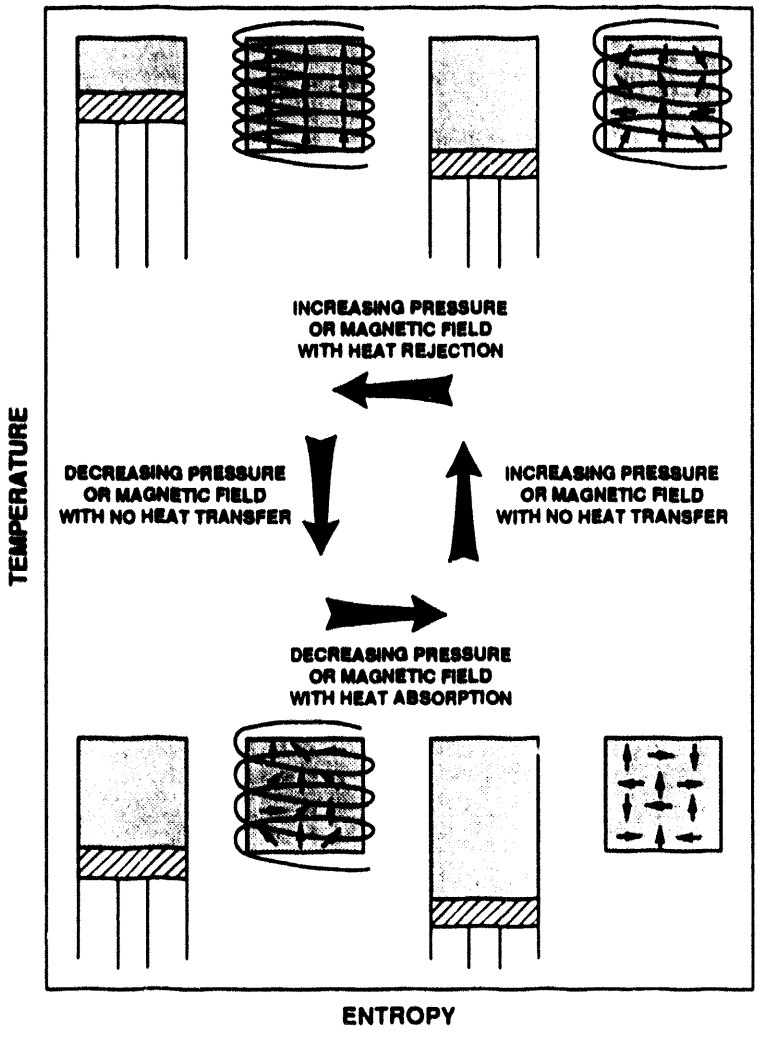

Fig. 2.1. The solid state cooling process used in magnetic refrigeration.

Energy Division evaluated alternate candidates and devised upper stage options to meet the stated interface requirements. Issues that were addressed in Task 1 include magnetocaloric refrigerant composition and configuration, magnetic field implementation and control, energy flows, and gas cycle refrigerator implementation. Based on the designs developed in Task 1, fabrication efforts comprise Task 2. The components created in Task 2 will be integrated and tested in Task 3.

Results

After facility modifications, tests with both the primary magnetocaloric material and alternatives were conducted on the Active Magnetic Regenerator Universal Test Apparatus. The primary material showed the capability to span the temperature range of 25 to 80 K with no refrigeration load and 40 to 80 K with a refrigeration load operating in an active magnetic regenerator cycle (Fig. 2.3). Good agreement was found between the experimental results and the performance model. Based on preliminary cycle performance analysis, a conceptual design was developed. With the magnet size, shape, field, and protection requirements from the conceptual design, magnet design analysis was performed to characterize winding specifications, flux return options, force predictions, and heat leak/Dewar implications for a magnet system employing available low-temperature superconductors. Based on the heat rejection requirements of the magnetic (low-temperature) stage, surveys of available and developmental refrigeration systems for applicability to the high-temperature stage of the hybrid machine were conducted (Fig. 2.4). Realistic high-temperature stage options and tradeoffs were summarized, and low-temperature/high-temperature stage interface requirements were established. With the best available information, a preliminary design for the

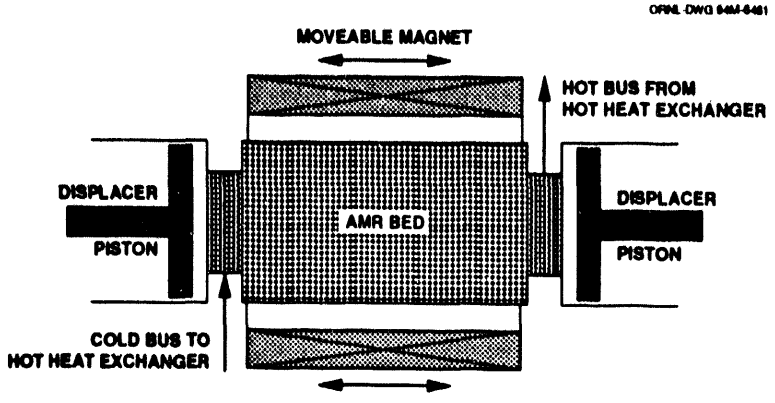

Fig. 2.2. Active magnetic regenerator.

performance improvements from the implementation of layered beds were identified as remaining issues. Additional tests and analyses were performed to resolve these in preparation for peer review presentation and critical design review. Based on the resulting final design, associated specification packages were created and procurement actions were initiated. Fabrication and component-testing activities

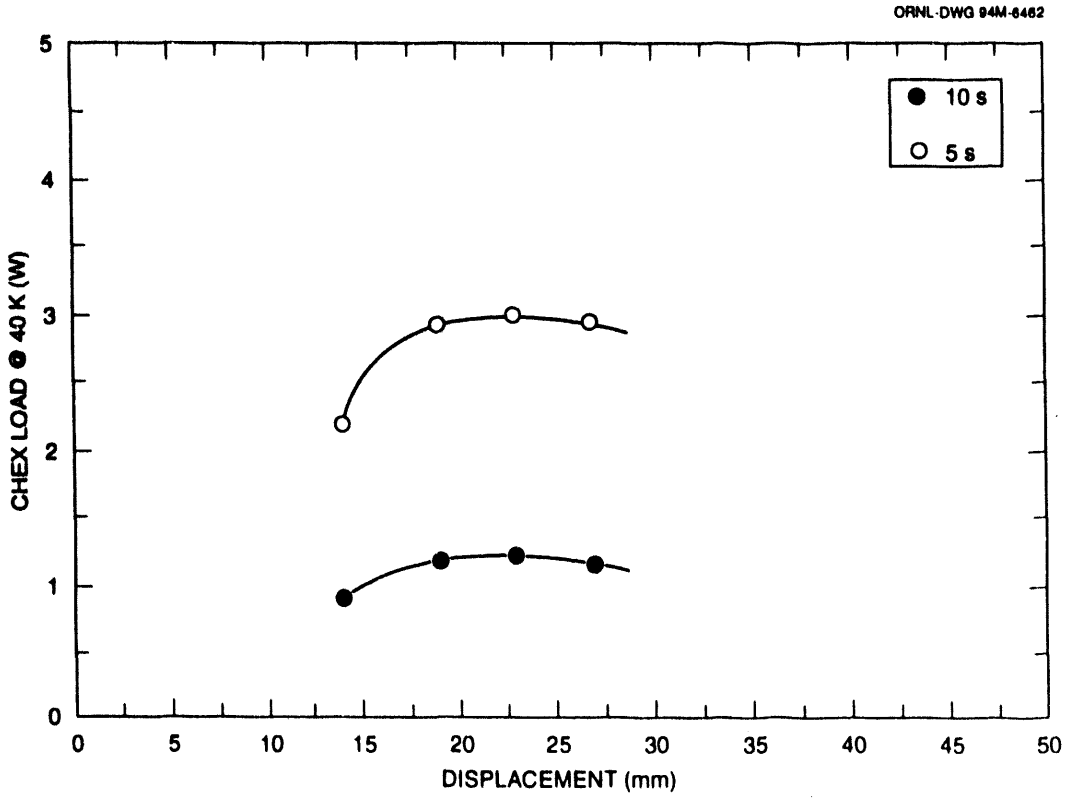

Fig. 2.3. Test results from use of primary magnetocaloric material (7 T, 15 atm) in the Active Magnetic Regenerator Universal Test Apparatus.

refrigerator was developed. As a result of the preliminary design review, magnetic material particulation techniques and possible bed degradation, reliability in sealing situations involving hoses and bellows, and potential continued through the end of FY 1993.

The major technical achievements of this project to date are (1) development of mechanical, thermal, magnetic, and thermodynamic system models to provide a

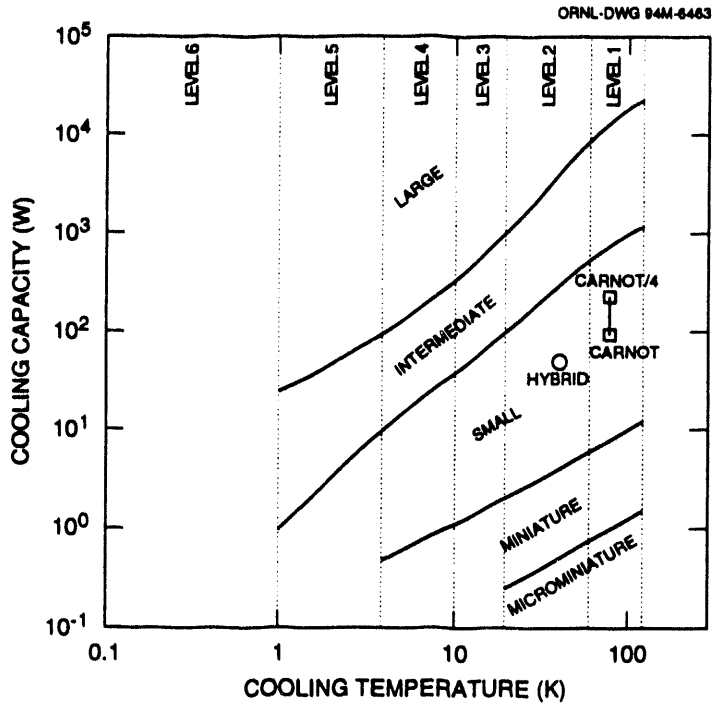

Fig. 2.4. Level and size map for cryocoolers.

basis for option evaluation and design; (2) modification and successful extended operation of the Active Magnetic Regenerator Universal Test Apparatus in relevant ranges; (3) identification and resolution of critical magnetic refrigerator design issues through supplementary testing and analysis; (4) evaluation and specification of magnet design options to meet field requirements consistent with protection, loss, and force considerations; (5) characterization of upper stage options to meet lower stage heat rejection requirements for a hybrid unit; (6) creation and review of final design and associated specification packages; and (7) initiation of fabrication and component-testing activities.

FY 1994 Plans

Verified components and subsystems will be assembled and integrated to form the refrigerator system. Shakedown tests will be conducted to identify unforeseen problems or nonconformities. Upon successful resolution of these, performance mapping of the system will ensue. Resulting data will be compared with model predictions, and appropriate modifications will be attempted.

HIGH-TEMPERATURE SUPERCONDUCTOR COIL DEVELOPMENT FOR ELECTRIC POWER APPLICATIONS

Our work in FY 1993 was mainly carried out in collaboration with three U.S. industries: American Superconductor Corporation (ASC), Intermagnetics General Corporation (IGC), and Reliance Electric Company (REC). It comprised five main activities: measurements of small high-temperature superconductor coils, theoretical calculations concerning the stability and protection of such coils, information and testing to help select insulation and bobbin materials, provision of cryogenic engineering assistance, and measurement to evaluate a particular winding method.

Measurements as a function of temperature over the range from 4.2 to 110 K in background fields from 0 to 5 T were made on small high-temperature superconductor coils supplied by both ASC and IGC (Fig. 2.5). IGC used the wind-and-react method, while ASC continues to champion the react-and-wind method. The best coils of each manufacturer carried close to 15 A at 4.2 K with no background field superimposed. The ASC coil wound with Bi-2223 material indicates that the temperature range of useful current density at

ORNL PHOTO 3672-93

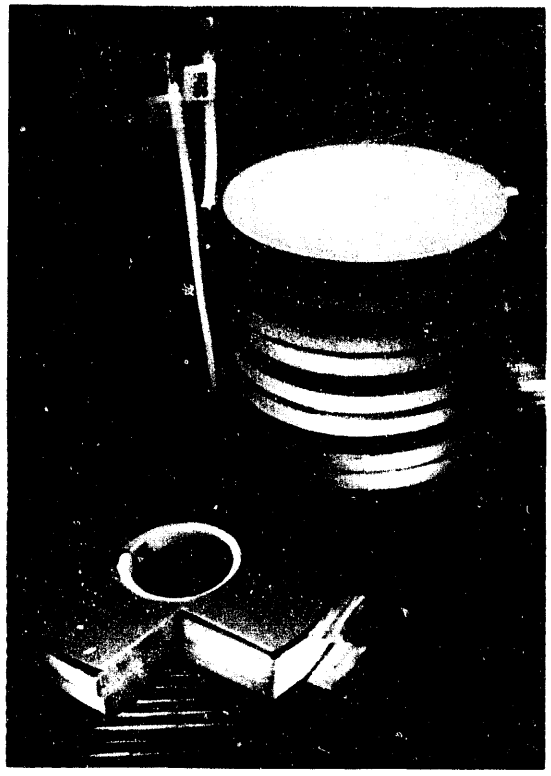

Fig. 2.5. High-temperature superconductor coil.

high fields may be extended to 50 K instead of the previous limit of 30 K. Measurements on a coil with a new high-temperature superconductor material, Y-124, were performed with not as favorable results as the Bi-2223 material. The voltage power law in the flux flow regime shows that the Bi-2223 material is about twice that of the Y-124. As with the critical current, the *n*-value drops rapidly with the initial field increase of a few tenths of tesla (Figs. 2.6 through 2.8).

Ramped field measurements on an IGC coil with multiple in-hand turns were extended to lower temperatures (down to 4.2 K with higher ramp rates) and as large as 2.5 T/s (Figs. 2.9 through 2.11). The eddy currents were still low enough to be of no concern. The new IGC coils contained longer lengths of BSCCO material and also had higher current densities than those produced last year. One IGC coil was measured both in helium gas and in pumped LN_2 coolant over the temperature range of 65 to 77 K with no difference in the results. Steady improvement in the critical current density was noted during the year. At the end of the year, the critical current was a factor of 2.7 higher than the initial coils measured at all temperatures.

A program was also carried out for ASC on selection of insulation, potting material, and bobbin preparation. Candidate material was selected at ORNL and sent to ASC for their evaluation. ASC then selected material that passed their test. The priorities for the potting material are the coefficient of thermal expansion (CTE), thermal cycling, adhesion to the insulation material, the curing temperature, and bonding to the bobbin material. The primary measurements conducted at ORNL are the CTE and the mechanical measurements. The baseline insulation and bobbin material were selected, and the surface preparation needed for the bobbin material has been determined.

Other cryogenic calculations were carried out to support the REC design activity. We supplied cryogenic materials data and superconducting motor and generator literature to engineers working on the superconducting motor project. The cryogenic aspects of the motor design were reviewed, and we made suggestions on a demountable flange for a rotating cryostat.

The theoretical work mainly in support of the motor project at REC consisted of three papers accepted for publication. One extended the calculation of the propagation velocity without the restriction of temperature operation to 20 to 40 K, since REC intends to operate motors in liquid nitrogen. The voltage of a propagating normal zone was calculated and compared with the hot spot temperature. The normal zone voltage is detectable before the conductor overheats and is damaged. A second paper concerns the quench energy

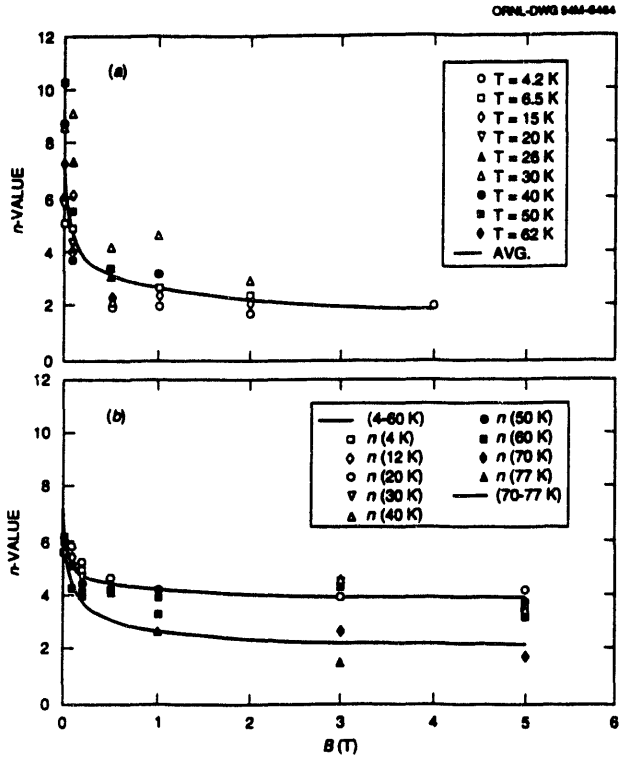

Fig. 2.6. *n*-value as a function of external field: (*a*) Y-124 coil; (*b*) Bi-2223 coil.

needed to initiate a propagation also without restriction to the temperature range of 20 to 40 K. This should be compared with the perturbation introduced by shaft seizure in motors. This paper showed that the stability of high-temperature superconductor magnets is sufficiently high that no training of potted magnets will occur. The final paper concerns the stability of an uncooled segment of a high-temperature superconductor coil and calculates the steady states that are possible. The loss of coolant (by level drop or vapor lock) is always a possibility in any application, particularly motors, and must be considered for a complete understanding of the safety issue.

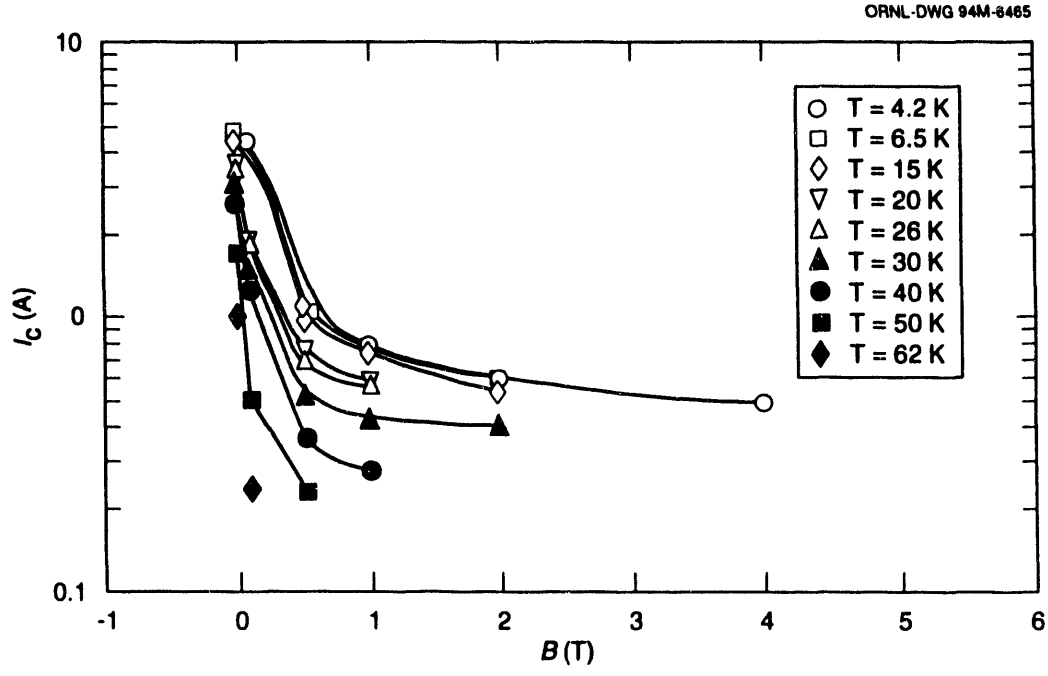

Fig. 2.7. Critical current as a function of magnetic field at different temperatures for a small coil made of Y-124 superconductor by American Superconductor Corporation.

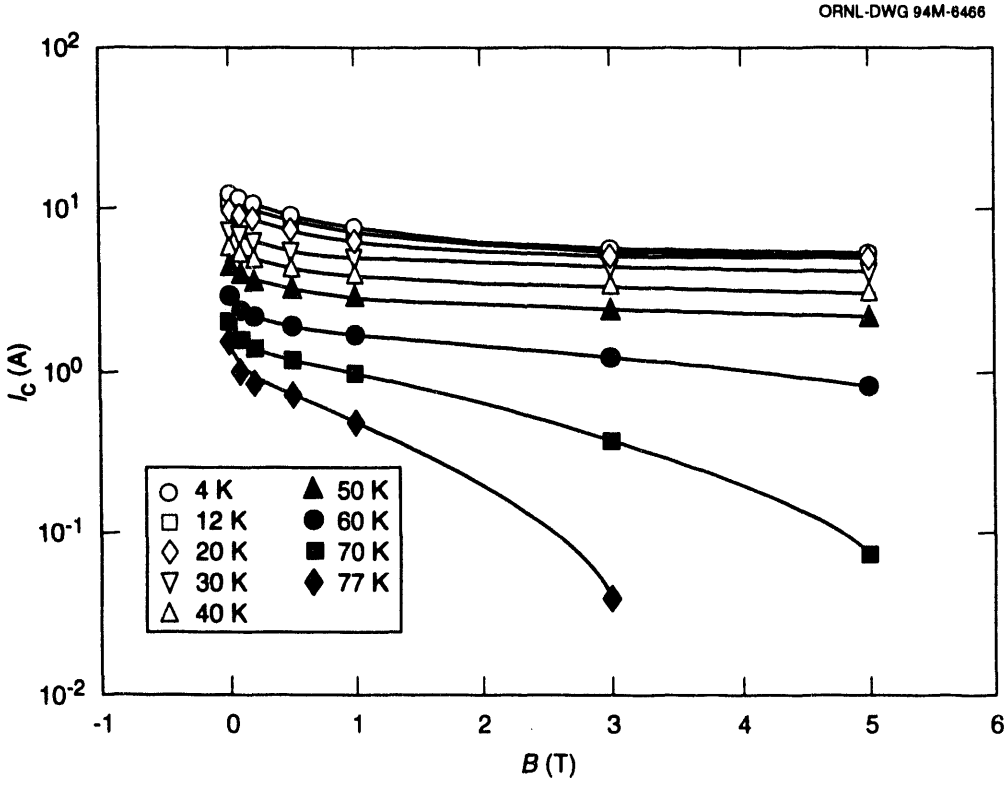

Fig. 2.8. Critical currents as a function of magnetic field at different temperatures of a small solenoid coil made of Bi-2223 superconductor by American Superconductor Corporation. I_c decreases slowly and exponentially with increasing B for fields above 0.5 T at temperatures up to 50 K. Bigger drops in I_c were seen only at temperatures above 60 K.

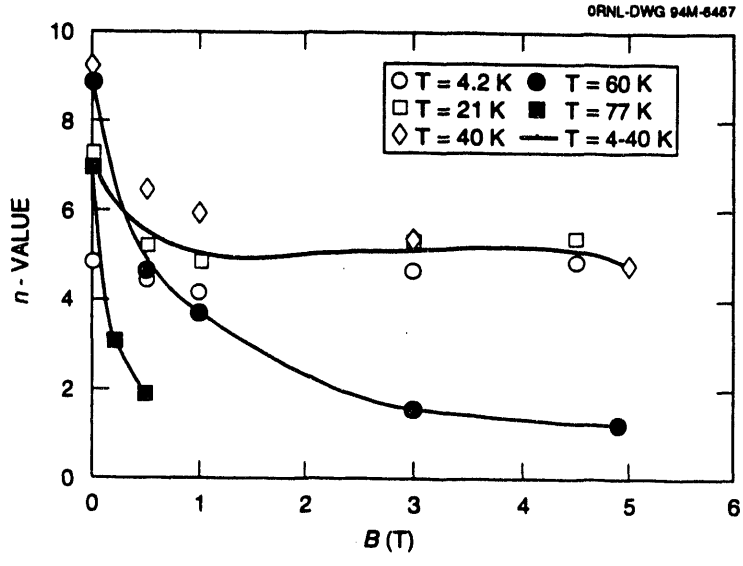

Fig. 2.9. Intermagnetics General Corporation coil test results (No. 3, n vs B).

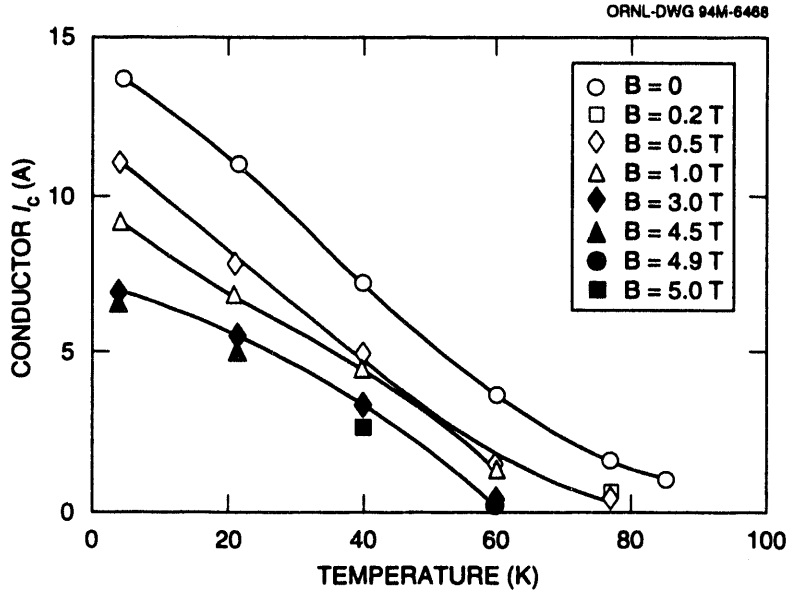

Fig. 2.10. Intermagnetics General Corporation coil test results (No. 3, I_c vs T).

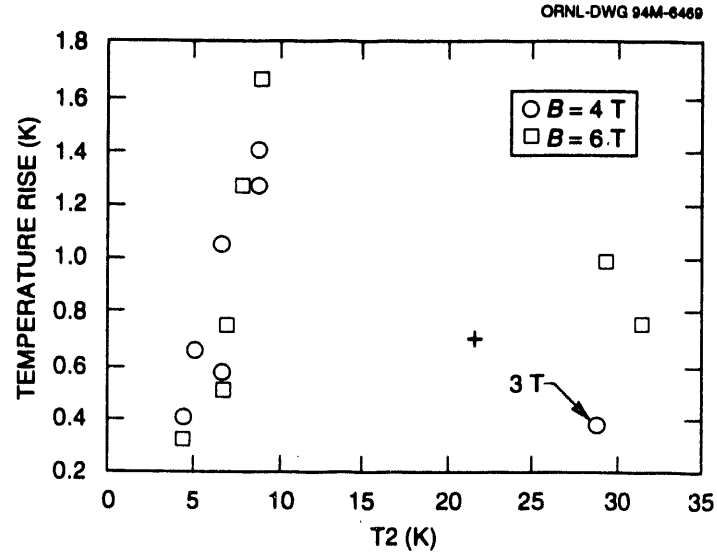

Fig. 2.11. Temperature rise due to eddy current heating in ramped fields of 2.5 T/s (not significant in operating area of interest 4.2 K or above 20 K).

The background magnet facility upgrades resulted in safer operation of the motor generator sets and permitted higher background fields. Another benefit is much better signal-to-noise ratios in low-background fields. This will permit more accurate determination of the critical current at very small values.

Summary of Technology Transfer Activities

BACKGROUND

Oak Ridge National Laboratory (ORNL) is a key part of the U.S. Department of Energy's (DOE's) national effort on electric power applications of high-temperature superconductivity. ORNL has formed effective teams that combine the resources of the Laboratory with the entrepreneurial drive of private companies. New technology transfer methods, a feature of the ORNL Superconducting Technology Program for Electric Power Systems since its inception in 1988, have resulted in 27 superconductivity cooperative research and development agreements. In addition, licensing agreements, joint inventions, and joint publications with the private industry partners have ensured that there is technology transfer throughout the program.

Technology transfer on Laboratory-industry teams may occur in several ways. "Spinoff" technology transfer involves the license of patentable Laboratory inventions to industry, continued product or process development of the point of demonstration of commercial viability, or both. Licensing of Laboratory spinoff technologies is how the "spectator" can participate in this national program. However, this type of technology transfer is the traditional one-way variety in which the Laboratory invents and private industry applies. In this program the cooperative development level of technology transfer is emphasized: joint industry-Laboratory teams work on a problem that requires combined resources and expertise with a clear objective of industry commercialization of the results of the work. For the project to succeed, each partner depends on the success of the other.

Most of the industrial competitiveness projects with private industry, and much of the Laboratory precompetitive research and development work, are developing key technology in which commercialization of the results is expected to occur after a minimum of 3 to 5 years. Some activities are also of a higher risk, longer term nature for which new markets, or a shift of markets, to embrace high-temperature superconductivity are expected if the project succeeds. For example, several companies continue to search for innovative ways to apply YBCO in the manufacture of long lengths of wire. This wire may still be the only option for practical performance levels in high magnetic fields at temperatures greater than 77 K.

RELATIONSHIP TO THE DOE MISSION

The ORNL program mission is that of its program sponsor, DOE's Office of Energy Management, Advanced Utility Concepts Division: to develop the technology base necessary for industry to proceed to commercialization of electric energy applications of high-temperature superconductivity. High-temperature superconductivity will enable new energy-efficient motors, generators, and transmission lines and will also provide electric power equipment manufacturers with strategic technology for global competitiveness. Electric utilities can defer acquisition of new transmission rights-of-way with successful introduction of superconducting cables. System stability and protection will be enhanced with the introduction of fault current limiters. Distributed utility systems in the future, which will include distributed generation systems, will benefit from the smaller size and weight of the next generation of electric power equipment.

FUNDING

DOE funding for the program, together with subcontracting activities in 1993 and a summary of funds-out cooperative agreements, is shown in Tables 3.1 and 3.2 and in Fig. 3.1.

TECHNOLOGY TRANSFER APPROACH

Our interdisciplinary approach uses all resources available at ORNL to meet the program goals for joint industry/Laboratory development of high-temperature superconducting technology for electric power applications. Our superconductivity agreement mechanism interlinks research and development projects with industry and universities that optimize the utilization of facilities, expertise, and program resources for the benefit of all participants. This program also coordinates the ORNL activities with the other national Laboratories, government agencies, university centers, and industry groups including the Electric Power Research Institute (EPRI).

Cooperative agreements ensure that technology development is industry-driven. The Office of Guest and User Interactions and Patent Counsel work together to place these agreements. Where appropriate, these efforts are coordinated with projects within ORNL that are funded by the DOE Office of Energy Research, as well as Work for Others and ORNL Director's Research and Development Fund projects. Effective funds-out to industry is used to supplement industry cost share. In FY 1993 over $1 million funds-out to industry was provided through cooperative agreements and subcontracts. To keep industry involved from the start of the program and to ensure commercialization potential, these technology transfer mechanisms are augmented by CRADAs, user agreements, and licensing activities.

Responsiveness to American industry has high priority in this program. An ORNL ad hoc technical review committee, consisting of a program manager, a scientific coordinator, a manager for conductor development, and a manager for applications development, reviews all inquiries from

Table 3.1. Superconducting Technology Program funding: authorization and outlay

	New budget authorization/outlay ($ × 1000)			
	FY 1989/1990	FY 1991	FY 1992	FY 1993
Direct scientific and technical[a]	2072	3146	3213	3511
Management and outreach	230	219	280	294
Subtotal ORNL	2302	3365	3493	3805
Subcontracts[b]	0	154	439	428
Funds-out cooperative agreements	1068	681	1072	867
Total program	3370	4200	5004	5100

[a]See Fig. 3.1 for distribution of funding for Oak Ridge National Laboratory.

[b]Details are provided in separate tables. Funds-out cooperative agreements provide direct financial support to U.S. industry for cost-shared cooperative research and development.

Table 3.2. Summary of funds-out cooperative agreements: January 31, 1994

Participant	Approved term	Type[a]	Total agreement cost share ($× 1000)			Technology area
			By DOE to ORNL	By DOE to industry	By industry	
Advanced Fuel Research (C)[b]	2/1/90–9/30/92	NFE	230	0	442	In situ deposition monitor
American Magnetics (C)	8/10/89–8/9/92	NFE	100	0	480	Char. of MOCVD-deposited multifilament conductors
American Superconductor	9/1/91–11/15/95	FO	575	350	405	Coil fabrication, technology development, and testing
American Superconductor	9/1/91–11/15/95	NFE	1615	0	1252	Fabrication of powder-in-tube wire and tape
Astronautics	9/1/91–8/31/94	FO	600	450	820	Magnetic refrigeration
CeraNova Corporation	8/1/93–1/31/95	FO	40	25	25	Melt-processed YBCO wire for leads and coils
Consultec Scientific (C)	6/1/89–12/31/90	FO	38	45	64	Deposition target device
Corning	6/1/89–12/31/93	FO	325	275	316	Deposition on flexible ceramic substrates
CPS Superconductor (C)	4/1/91–3/31/93	NFE	80	0	50	Conductor fabrication—continuous filament melt-textured YBCO
Dow Corning (I-IIa) (C)	7/1/90–9/30/91	FO	110	50	67	Thick film deposition
DuPont (C)	7/1/89–3/31/91	NFE	225	0	250	Thin film devices and bulk applications
Electric Power Research Institute	7/13/93–7/12/96	CR	190.5	0	214.9	Variable speed superconducting motors, power electronics, and SMES
Energy Conversion Devices (C)	5/1/91–3/31/93	NFE	90	0	90	Deposition of conductors
General Electric (A1) (C)	12/15/88–2/28/89	FI	5	0	45	Thallium HTS material processing
General Electric (B1)	10/1/89–12/31/94	FO	670	420	514	Laser deposition of conductors; thallium-deposited conductors
General Electric (C1) (C)	4/1/90–12/31/90	NFE	135	0	140	Thallium HTS material processing
HiTc Superconco (C)	3/1/90–4/30/91	NFE	40	0	50	Magnetic bearings

Table 3.2 (continued)

Participant	Approved term	Type[a]	Total agreement cost share ($× 1000)			Technology area
			By DOE to ORNL	By DOE to industry	By industry	
Innovative Materials Technology (C)	10/1/89–3/31/90	FI	50	0	50	Composite tape fabrication
Intermagnetics General Corporation	10/1/91–9/30/94	FO	250	290	256	Coal fabrication and testing; BSCCO 2212 tapes
Intermagnetics General Corporation	9/1/91–8/31/95	NFE	300	0	300	Thallium powder-in-tube conductor
International Business Machines	2/1/90–1/31/93	NFE	255	0	673	Optimize flux pinning via ion-induced defects
International Business Machines	2/1/90–5/31/93	FO	201	389	186	Optimize flux pinning via ion-induced defects
Neocera (C)	2/1/91–1/31/93	FO	80	111.6	95.7	Laser ablation multitarget deposition
Plastronic, Inc.	10/22/93–9/30/95	NFE	50	0	100	Apply wire-forming technology to produce BSCCO wire
Saphikon	2/1/92–1/31/94	NFE	50	0	492	Deposited conductor fabrication
SUNY–Buffalo (C)	7/1/89–10/30/92	FO	165	250	255	Laser deposition of conductors
Stevens Institute of Technology (C)	1/1/90–5/31/92	FO	90	105	100	MOCVD deposition for electronic devices
Superconductivity, Inc. (C)	10/1/89–3/31/93	NFE	180	0	133	Magnetic energy storage for end-use applications
Textron Specialty Materials (C)	8/1/89–3/31/91	NFE	60	0	45	Deposition of conductors
University of Wisconsin–Madison	8/1/92–9/30/94	FO	100	40	100	Aerosol powder synthesis
Westinghouse Electric	4/1/89–12/31/93	FO	1200	750	800	Powder scale-up, BSCCO wire fabrication, and leads
Total			8099.5	3550.6	8810.6	

Table 3.2 (continued)

Participant	Approved term	Type[a]	Total agreement cost share ($\times$ 1000)			Technology area
			By DOE to ORNL	By DOE to industry	By industry	
			Agreements in negotiation			
General Electric	12/1/93-11/30/95	NFE	400	0	1173	Superconductivity Partnership Initiative tasking—thallium wire development and generator design
Oxford Instruments	1/94-12/94	C	50	0	75	Develop technology for dip-coated BSCCO-2212 wire
			FY 1993/94 Subcontracts			
University of New Mexico	4/1/93-3/31/94			45		Study the generation of Pb-Bi-Sr-Ca-Cu-O (BSCCO) powders by aerosol decomposition
H. Hsu	11/15/93-11/14/94			48		Material synthesis and conductor fabrication
University of Tennessee	4/1/93-11/30/93			58		Advanced analytical electron microscopy techniques for HTS conductors
Georgia Institute of Technology	4/15/93-4/14/94			20		Study of combustion pyrolysis method for processing YBCO superconductors
National Institute of Standards and Technology (via Interagency Agreement)	8/93-7/94			100		BSCCO and TBCCO phase diagram support

[a]NFE—no funds exchange; FO—funds out; FI—funds in; CR—CRADA.
[b]Completed.

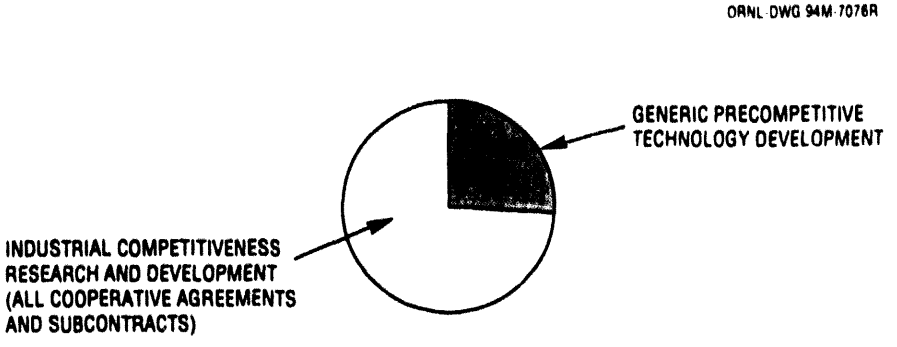

Fig. 3.1. ORNL funding distribution: FY 1993 new budget authorization and outlay.

industry and recommends a project for possible funding. This review ensures that (1) the proposed work fits the program mission, (2) the work is collaborative, (3) there is legitimate commercial interest, and (4) the work is feasible. Substantial private sector cost share is required on cooperative agreements.

ORNL provides support to the DOE Headquarters (DOE-HQ) Superconductivity Program for Electric Power Systems by identifying, guiding, and monitoring research and development at ORNL and ORNL subcontractor sites and by performing coordination, analysis, and planning of activities related to the national program. Some of the various activities performed as part of this task include:

- technical, program, and budget guidance;
- project identification and development;
- exploratory research and development;
- support of consultants and subcontracts providing technical, program, or technology transfer support;
- identification, placement, and technical monitoring of subcontractors, review committee members, and workshop guests;
- guidance and support on technology transfer;
- publication of reports and proceedings from workshops;
- identification and initiation of cooperative agreements, interagency agreements (i.e., National Institute of Standards and Technology), and Memoranda of Understanding;
- distribution of reports to program managers;
- coordination of the Laboratories' Industrial Overview Committee;
- preparation of assessments to address technical, economic, regulatory, and institutional issues in the DOE program;
- coordination of interlaboratory technical team meetings;
- assistance to the DOE-HQ program manager and Energetics in preparation of the Superconducting Technology Program Annual Operating Plan;
- assistance in the open annual review meeting preparations and contracting;
- collection and dissemination of programmatic information and program-wide assessments;
- coordination of Superconducting Technology Program workshops (one per year), including all subcontracting required for guest speakers and workshop arrangements; and
- review of industrial collaboration opportunities through multi-Laboratory meetings and conference calls.

ORNL works with the other program Laboratories to address issues such as communication among program participants, workshop and meeting implementation, planned competitive solicitations and superconductivity agreements, and coordination of technical and economic assessments. ORNL manages the Energetics subcontract and is developing a program annual operating plan.

An Industrial Overview Committee is charged with reviewing program activities and advising Laboratory management as to program progress, policy, and direction. The committee consists of representatives of electric utilities, original equipment manufacturers, and high-temperature superconducting wire manufacturers. This committee meets twice a year at ORNL, Argonne National Laboratory, or Los Alamos National Laboratory.

PROGRAM MEASURES

Four new cooperative agreements were executed during FY 1993: Saphikon, the University of Wisconsin-Madison, EPRI, and CeraNova Corporation. New Statements of Work were negotiated, and agreements were extended with American Superconductor Corporation, Intermagnetics General Corporation, General Electric Company, International Business Machines, and Westinghouse Electric Corporation. In addition, four new agreements, including one with General Electric Company to support their Superconductivity Partnership Initiative Team, were under negotiation in early FY 1994.

Six new invention disclosures were submitted by ORNL or industry principal investigations. These are listed in Table 3.3 together with all others for the program.

PROGRAM HIGHLIGHTS

Additional highlights of program activities include the first license of program-developed technology for a private company, use of the mechanical properties microprobe (MPM) at the High-Temperature Materials Laboratory user facility, and numerous publications and presentations with industry partners.

Licensing of Superconducting Wire Technology

Energy Systems signed a license agreement with Superconductive Components, Inc. (SCI), a Columbus, Ohio, firm, to commercialize the ORNL superconducting wire manufacturing technology. ORNL researchers D. M. Kroeger and J. Brynestad and ORNL consultant H. Hsu developed a process for producing superconducting powder precursors of BSCCO. The product is an oxide metal powder that can be doped with lead to improve its properties. The process can produce lead-doped powders without measurable lead loss. The distribution of the particle sizes is narrow (i.e., from 0.1 to 1.0 μm).The grain size within a particle is very fine, and the chemical homogeneity from grain to grain is good.

The process is scaleable to high-powder production rates. SCI will further develop the process to produce powders for sales and for use in bearings, current leads, superconducting wire, and magnetic levitation demonstrations. E. R. Funk, president of SCI, stated, "The licensing of the ORNL BSCCO process completes our line of high-quality superconductive powders. The ORNL process is an important technological advance in tailoring the BSCCO powder for specific applications."

According to R. A. Hawsey, director of ORNL's High-Temperature Superconductivity Program, "The commercialization of this process will benefit American industry as a whole. The increased quality and availability of the BSCCO powders may make possible large-scale products."

Table 3.3. Superconducting Technology Program invention disclosures

ESID	Subject of disclosure	Submitted by
935-X	"Method for Fabricating Continuous Ribbons of High Temperature Superconductors"	V. K. Sikka and C. E. Dunn (ORNL)
1018-X	"Improved $Y_1Ba_2Cu_3O_7$ Superconductor"	A. D. Marwick and L. Civale (IBM), and J. R. Thompson (ORNL)
964-X	"Chemically Compatible Substrate/Jacket Alloy for Oxide Superconductors"	D. M. Kroeger, F. A. List III, and J. Brynestad (ORNL)
1039-X	"Method for Preparation of $(Bi\text{-}Pb)_2Sr_2Ca_2Cu_3$ Oxide Powders"	D. M. Kroeger, J. Brynestad, and H. S. Hsu (ORNL)
1040-X	"Method for Preparing Superconducting Wires from Oxide Powders"	D. M. Kroeger and H. S. Hsu (ORNL)
1058-X	"Rolled Current Density, High Temperature Ribbon Superconductors from Stacked Predeposited Strips"	G. A. Whitlow and J. C. Bowker (Westinghouse) and D. M.Kroeger and F. A. List III (ORNL)
1131-X	"Method of Forming Superconducting Joints Between Tapes of Oxide Superconductors" (87X-SE934V)[a]	R. H. Arendt and K. W. Lay (GE)
1155-X	"Method for Fabricating High Current Density, Oxide Superconductor Ribbons" (HTSPC-001)[a]	V. K. Sikka (ORNL)
1124-X	"Improved, Strain Tolerant High Temperature Superconductor" (87X-SD925C)[a]	G. A. Whitlow and W. R. Lovic (Westinghouse)
1129-X	"An Improved Heat Treatment for Composite Conductors Using $Bi_2Sr_2CaCu_2O_7$ Superconductor Material" (87X-SD925C)[a]	J. C. Bowker and G. A. Whitlow (Westinghouse)
1193-X	"Process for Fabricating Continuous Lengths of Superconductor" (86X-SD925C)[a]	D. M. Kroeger and F. A. List III (ORNL)
1233-X	"High Current Density, High Temperature Superconductors by Deformation of High Density Materials" (87X-SD925C)[a]	G. A. Whitlow, W. R. Lovic, and J. C. Bowker (Westinghouse), D. M. Kroeger and F. A. List III (ORNL)
1185-X	"Bipolar Pulse Field for Magnetic Refrigeration"	M. S. Lubell (ORNL)
1384-X	"Process to Enhance Superconducting Phase Formation, Grain Alignment, and Fracture Properties of High Temperature Superconductors"	V. Selvamanickam and D. M. Kroeger (ORNL)
1450-X	"Improved Efficiency High T_c Superconducting Magnet Lead Materials"	R. K. Williams (ORNL)
1467-X	"Superconducting Structure and Method for Making Same"	R. K. Williams and J. Brynestad (ORNL)
1471-X	"HTS Coil Grading to Compensate for Anisotropic Behavior of HTS Conductor"	D. Aized and R. Schwall (American Superconductor Corporation)

[a]Numbers in parentheses are cooperative agreement numbers under which the work was conducted.

Nanoindenter at ORNL's High-Temperature Materials Laboratory

The High-Temperature Materials Laboratory at ORNL has a nanoindenter, or MPM, that can provide unique insights into the mechanical properties of superconductors. The nanoindenter is a sophisticated version of a standard hardness tester. A hardness tester presses a sharp point (e.g., a four-sided diamond pyramid) against a sample of material. The point, loaded with a known mass in the range of a few grams to a kilogram, will make an indentation in the material. By studying the depth of the indentation as a function of the force on the point, researchers can determine the material's hardness and stiffness (i.e., elastic modulus).

The MPM is designed to operate with high sensitivity in the low-force regime. In its most sensitive mode it operates with loads in the microgram range and has a force resolution of 0.3 μN. Rather than measuring the indentations directly, the MPM calculates these based on the displacement of the point and the dimensions of the diamond indenter. It measures the position of the indenter relative to the surface by capacitive techniques with a vertical resolution of 2 Å. In the horizontal plane (the plane of the sample), the indenter can be positioned within 1 μm of any point on the specimen. The instrument can make a series of indents in any geometrical pattern, separated by steps as small as 1/10 μm.

The entire operation of the system is computer controlled. All these capabilities allow the instrument to characterize small volumes of material on an extremely localized scale. It is uniquely suitable for studying the mechanical properties of thin materials (e.g., films, coatings, and ion-implanted layers) or small secondary-phase particles within a larger sample.

A. Goyal and W. Oliver of ORNL have applied the nanoindenter to study the mechanical properties of melt-processed YBCO. "We looked at the anisotropy of the elastic modulus in melt-processed 123, which is a single crystal with second-phase 211 (Y_2BaCuO_5) inclusions," Goyal explained. "We wanted to measure the elastic modulus in the *c* direction and along the basal plane and also to study the effect of 211 particles on the mechanical properties of 123. That was the basic idea of the work."

The researchers next used the facility in collaboration with American Superconductor Corporation for studies of BSCCO powder-in-tube wire. "If you characterize the mechanical properties of all the phases in the wire and correlate those measurements with its overall texture and transport critical current density, you might learn how to optimize the deformation processing for improved textures and higher J_c. As far as I know, the nanoindenter is the only instrument with which you can study the mechanical properties of various phases in power-in-tube wire because of the fine scale of the microstructure," said Goyal.

Publications and Presentations

Figure 3.2 shows the total number of publications and presentations during FY 1993. A detailed listing is presented in the following section.

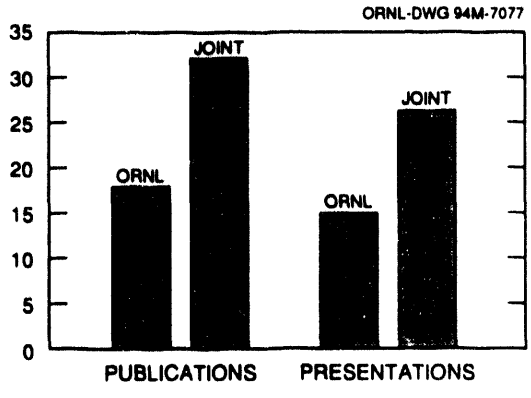

Fig. 3.2. FY 1993 publications and presentations.

FY 1993 Publications and Presentations

D. M. Kroeger, Z. L. Wang, and A. Goyal,[1] "Flux Pinning Structures in Melt-Processed $YBa_2Cu_3O_{7-x}$," submitted for publication in Proceedings of the Fifth U.S./Japan Workshop on High-T_c Superconductors, Tsukuba, Japan, November 1992.

G. A. Whitlow, J. C. Bowker, and W. R. Lovic,[2] "Development of High Critical Currents in Ag/2212 Wires and Tapes," submitted for publication in Proceedings of the Fifth U.S./Japan Workshop on High-T_c Superconductors, Tsukuba, Japan, November 1992.

F. A. List, H. Hsu, O. B. Cavin, W. D. Porter, C. R. Hubbard, and D. M. Kroeger,[1] "Phase Development in the $Bi_2Sr_2CaCu_2O_y$ System: Effects of Oxygen Pressure," *Physica C* **202** 134-40 (November 1992).

L. Dresner,[1] *Protection of a Test Magnet Wound With an Ag/BSCCO High-Temperature Superconductor*, ORNL/HTSPC-3, Martin Marietta Energy Systems, Oak Ridge National Laboratory, October 1992.

Z. L. Wang, R. Kontra, A. Goyal, and D. M. Kroeger,[1] "Microstructures and Flux-Pinning in Melt-Processed $YBa_2Cu_3O_{7-x}$," submitted to *Mater. Sci. Forum* (1992).

J. R. Thompson,[1] "Vortex Pinning by Line- and Point-Like Defects in High Temperature Superconductors," presented at Materials Research Society Fall Meeting, Symposium H, Boston, Mass., Nov. 30-Dec. 4, 1992.

H. R. Kerchner, J. R. Thompson, Y. R. Sun, D. K. Christen, and B. C. Chakoumakos,[1] J. O. Thomson,[3] and L. Civale and A. D. Marwick,[4], "Enhanced Critical Current Density and Magnetic Irreversibility Line in Single Crystal $Bi_2Sr_2CaCu_2O_8$ via Columnar Defects from Heavy Ion Irradiation," poster presented at Materials Research Society Fall Meeting, Boston Mass., Nov. 30-Dec. 4, 1992.

D. K. Christen, S. Zhu, C. E. Klabunde, R. Feenstra, J. R. Thompson, and H. R. Kerchner[1] and L. Civale and A. D. Marwick,[4] "Effects of Columnar Defects on the Superconducting Transport Properties of Epitaxial $Y_1Ba_2Cu_3O_7$ Thin Films," poster presented at Materials Research Society Fall Meeting, Boston Mass., Nov. 30-Dec. 4, 1992.

J. R. Thompson, Y. R. Sun, L. Civale, D. K. Christen, H. R. Kerchner, Y. J. Chen, B. C. Sales, B. C. Chakoumakos, A. D. Marwick, and F. Holtzberg,[4] "Effective Vortex Pinning Energy $U_{eff}(J,T)$ in High-T_c Superconductors with Point- and Line-Like Defects," abstract submitted to American Physical Society Meeting, Seattle, Wash., Mar. 22-26, 1993.

Y. R. Sun, J. R. Thompson, D. K. Christen, H. R. Kerchner, Y. J. Chen, C. E. Klabunde, B. C. Sales, and B. C. Chakoumakos,[1] L. Civale, A. D. Marwick, and F. Holtzberg,[4] "DC Magnetization Studies of Anisotropy in Heavy Ion Irradiated $Bi_2Sr_2Ca_1Cu_2O_8$ and $Y_1Ba_2Cu_3O_{7-\delta}$ Single Crystals," abstract submitted to American Physical Society Meeting, Seattle, Wash., March 22-26, 1993.

S. Zhu, D. K. Christen, C. E. Klabunde, J. R. Thompson, E. C. Jones, R. Feenstra, D. H. Lowndes, and D. P. Norton,[1] "Superconductive Transport Properties of Heavy Ion Irradiated Epitaxial $YBa_2Cu_3O_7$ Thin Films," abstract submitted to American Physical Society Meeting, Seattle, Wash., Mar. 22-26, 1993.

L. Dresner,[1] "Stability and Protection of Uncooled Magnets Wound with High-Temperature Superconductors," abstract submitted to the 13th International Conference on Magnet Technology, 1993.

S. Y. Lee, E. Narumi, and D. T. Shaw,[6] "Thermally Activated Dissipation in $Y_1Ba_2Cu_3O_{7-x}/Y_1Ba_2(Cu_{1-x}Ni_x)_3O_{7-x}$ Superconducting Multilayer Thin Films," *Physica C* **201**(3 and 4) (Dec. 10, 1992).

J. L. Routbort, S. J. Rothman, and J. N. Munday,[7] J. E. Baker,[8] B. Dabrowski,[9] and R. K. Williams,[1] "Oxygen Tracer Diffusion in $YBa_2Cu_4O_8$," submitted to *Phys. Rev. B* (1993).

J. E. Tkaczyk, J. A. DeLuca, P. L. Karas, and P. J. Bednarczyk,[10] and D. K. Christen, C. E. Klabunde, and H. R. Kerchner,[1] "Enhanced Transport Critical Current at High Fields after Heavy Ion Irradiation of Textured $TlBa_2Ca_2Cu_3O_z$," submitted to *Appl. Phys. Lett.* (1993).

E. C. Jones, D. K. Christen, and J. R. Thompson,[1] R. C. Dynes, S. Zhu, J. M. Phillips, and M. P. Siegal, "Effect of Current Percolation on the Superconducting Hall Transitions of Epitaxial Thin Films of $YBa_2Cu_3O_{7-\delta}$," *Physica C* (1993).

E. C. Jones, D. K. Christen, J. R. Thompson, J. G. Ossandon, R. Feenstra, J. M. Phillips, and M. P. Siegal, "Upper Critical Fields of $YBa_2Cu_3O_{7-\delta}$ Epitaxial Thin Films with Variable Oxygen Deficiency δ," *Phys. Rev. B* (1993), in press.

J. R. Thompson, Y. R. Sun, D. K. Christen, and H. R. Kerchner,[1] L. Civale, A. D. Marwick, and F. Holtzberg,[4] "Vortex Pinning in High-T_c Superconductors with Point- or Line-Like Defects: Experimental Tests of Theories for Pinning with Random or Correlated Disorder," abstract submitted to International Conference on Low Temperature Physics, Eugene, Oreg., August 1993.

J. C. Bowker and G. A. Whitlow,[2] "Effect of Heat Treatment Conditions on Critical Current of $YBa_2Cu_3O_{7-\delta}$/Ag Powder-in-Tube Wires," *Superconductor Sci. and Technol.* **6**(2), (February 1993).

D. M. Kroeger and A. Goyal,[1] "Critical Current and Microstructure in Oxide Superconductors," *J. Min., Met., and Mater. Soc.* (October 1992).

D. K. Christen, S. Zhu, C. E. Klabunde, J. R. Thompson, R. Feenstra,[1] L. Civale,[4] and J. M. Phillips, "Effects of Columnar Defects on the Superconducting Properties of $YBa_2Cu_3O_{7-\delta}$: Limits to the Irreversibility Line," submitted to *Physica B*, and abstract submitted for presentation to the LT20 Conference in Eugene, Oreg., Aug. 11-14, 1993.

H. R. Kerchner, J. R. Thompson, Y. R. Sun, D. K. Christen, J. O. Thomson, B. C. Sales, B. C. Chakoumakos,[1] and L. Civale and A. D. Marwick,[4] "Enhanced Vortex-Pinning Strength and Magnetic-Irreversibility Line via Columnar Defects in Single Crystal $Bi_2Sr_2CaCu_2O_8$," submitted to *Physica B*, and abstract submitted for presentation to the LT20 Conference in Eugene, Oreg., Aug. 11-14, 1993.

J. D. Budai, D. P. Norton, B. C. Chakoumakos, E. C. Jones, R. Feenstra, D. K. Christen, and D. H. Lowndes,[1] and R. T. Young,[5] "Epitaxial YBaCuO Films on Metal Substrates and Buffer Layers," presented at the Meeting of the American Physical Society, Seattle, Wash., March 22-26, 1993.

J. G. Ossandon, J. R. Thompson, D. K. Christen, Y. R. Sun, B. C. Sales, and H. R. Kerchner,[1] and J. E. Tkaczyk and K. W. Lay,[10] "Properties of Aligned $YBa_2Cu_3O_{7-\delta}$ Superconductor as a Function of Oxygen Deficiency δ," *Appl. Superconductivity J.* (special issue—Pt. 1), **1**(3-6) (March-June 1993).

A. Goyal,[1] "Microstructure and Processing of Thallium-Based Superconductors," presentation to Workshop on Tl-Based Superconductors, National Renewable Energy Laboratory, Golden, Colo., Feb. 25-26, 1993.

D. K. Christen,[1] "Limits to Critical Currents in High-Temperature Superconductors," presented at the Physics Department Colloquium at the University of Louisville, Feb. 12, 1993.

C. Vahlas and T. M. Besmann,[1] "Thermodynamics of the Y-Ba-Cu-C-O-H System: Application to the Organometallic Chemical Vapor Deposition of the $YBa_2Cu_3O_{7-x}$ Phase," *J. Amer. Ceram. Soc.* **75**(10), 2679-86 (October 1992).

J. R. Thompson, Y. R. Sun, D. K. Christen,[1] and L. Civale, A. D. Marwick, and F. Holtzberg,[4] "Vortex Dynamics in YBaCuO Single Crystals with Point- and Line-Like Defects—Flux Creep Studies," submitted to *Physica A* (1993).

J. R. Thompson, Y. R. Sun, D. K. Christen,[1] L. Civale, A. D. Marwick, and F. Holtzberg,[4] "Observed Regimes of Collective Flux Creep in Proton-Irradiated, Single Crystal YBaCuO: Dependence on Current Density," submitted to *Phys. Rev. Lett.* (1993).

Z. L. Wang, J. Brynestad, D. M. Kroeger, Y. R. Sun, J. R. Thompson, and R. K. Williams,[1] "Grain Boundary Chemistry and Weak-Link Behavior of Polycrystalline $YBa_2Cu_4O_8$," paper submitted to *Phys. Rev. B* (1993).

J. R. Thompson and D. K. Christen,[1] "Equilibrium Magnetization of the High-T_c Superconductor $Tl_2Ca_2Cu_3O_{10+\delta}$ and Fluctuation Effects," submitted to *Physica B* (1993).

Z. L. Wang, A. Goyal, R. Kontra, D. M. Kroeger, J. R. Thompson, and R. K. Williams,[1] "Microstructures of YBCO Superconductors and Ceramic Surfaces Determined by HRTEM and Associated Analytical Techniques," presented to NIST staff on May 21, 1993.

Z. L. Wang, J. Bentley, R. E. Clausing, A. Goyal, D. M. Kroeger, L. Heatherly, L. L. Horton, J. R. Thompson, and R. K. Williams,[1] "Microstructures of YBCO Superconductors and As-Grown CVD Diamond Films Studied by Analytical Electron Microscopy," presented to General Electric Central Research and Development staff on May 25, 1993.

A. Goyal, K. B. Alexander, and D. M. Kroeger,[1] and P. D. Funkenbusch, and S. J. Burns,[11] "Solidification of $YBa_2Cu_3O_{7-\delta}$ from the Melt," *Physica C* **210**, 197 (May 15, 1993).

E. D. Specht, A. Goyal, D. M. Kroeger, and Z. L. Wang,[1] and J. E. Tkaczyk and J. A. DeLuca,[10] "Observation of Local In-Plane Orientational Order in Polycrystalline $Tl_1Ba_2Cu_3O_x$ Films," abstract submitted to Symposium H: Superconductivity, Materials Research Society Fall Meeting, Boston, Mass., Nov. 29-Dec. 3, 1993.

R. K. Williams,[1] "High Pressure Studies," presentation to DOE/NIST Phase Diagram Workshop, Santa Fe, N.M., June 2-4, 1993.

L. Civale and A. D. Marwick,[4] R. Wheeler IV and M. A. Kirk,[17] and W. L. Carter, G. N. Riley, Jr., and A. P. Malozemoff,[12] "Superconducting Current Density Enhancement by Heavy Ion Irradiation of Bi-2223 Silver-Clad Tapes," *Physica C* **208**, 137-42 (1993).

Z. L. Wang, J. Brynestad, D. M. Kroeger, Y. R. Sun, J. R. Thompson, and R. K. Williams,[1] "Oxygen Content and Hole Density at Grain Boundaries in $YBa_2Cu_4O_8$ and their Relationship to Weak-Link Behavior," abstract submitted to Materials Research Society Symposium H: Superconductivity, Materials Research Society Fall Meeting, Nov. 29-Dec. 3, 1993.

Z. L. Wang, A. Goyal, and D. M. Kroeger,[1] and J. A. DeLuca and C. L. Briant,[10] "Grain Boundary Chemistry and Intragranular Defects in Spray-Pyrolyzed Tl-1223 Films," abstract submitted to Symposium H: Superconductivity, Materials Research Society Fall Meeting, Nov. 29-Dec. 3, 1993.

V. Selvamanickam[1] and M. Mironova, S. Son, B. C. Meyer, and K. Salama,[13] "Formation and Phase Decomposition of Textured $YBa_2Cu_4O_8$ Superconductor," abstract submitted to Symposium H: Superconductivity, Materials Research Society Fall Meeting, Nov. 29-Dec. 3, 1993.

M. Paranthaman, J. R. Thompson, Y. R. Sun, J. Brynestad, and D. M. Kroeger,[1] "Evidence for Phase Stability and Weak Links in Polycrystalline $HgBa_2CuO_{4+\delta}$," paper presented at DOE/NIST Phase Diagram Workshop, Santa Fe, N.M., June 2–4, 1993; and submitted for publication to *Appl. Superconductivity J.*, June 1993.

J. W. McKeever, C. W. Sohns, S. W. Schwenterly, R. W. Young, Sr., V. W. Campbell, M. H. Hickey, and G. W. Ott,[1] and J. M. Bailey,[3] "Operation of a Test Bed Axial-Gap Brushless DC Rotor with a Superconducting Stator," presented at the Cryogenic Engineering Conference/International Cryogenic Materials Conference, Albuquerque, N.M., July 1993.

M. Paranthaman,[1] and A. M. Hermann,[14] "Thallium-Based High-T_c Superconducting Oxides—A Summary," in *Organic Conductors: Fundamentals and Applications*, ed. J. P. Farges, Marcel Dekker, New York, 1993.

D. W. Yarbrough and R. K. Williams[1] and D. R. Shockley,[15] "Thermal Conductivities, Electrical Resistivities, and Seebeck Coefficients of $YBa_2Cu_3O_{7-x}$ Superconductors from 80 to 300 K," abstract submitted to the 22nd International Thermal Conductivity Conference, Tempe, Ariz., Nov. 7–10, 1993.

J. R. Thompson, Y. R. Sun, M. Paranthaman, J. Brynestad, and D. K. Christen,[1] "Vortex Pinning, Supercurrent Decay, and Weak Links in the Hg-Based High T_c Material $Hg_1Ba_2Cu_1O_{4-\delta}$," abstract submitted to Symposium H: Superconductivity, Materials Research Society Fall Meeting, Nov. 29–Dec. 3, 1993.

H. R. Kerchner, J. R. Thompson, Y. R. Sun, D. K. Christen, J. O. Thomson, J. Abell, and T. Armstrong,[26] and F. Holtzberg,[1] "Magnetic Irreversibility Range in Differing $YBa_2Cu_3O_{7-\delta}$," abstract submitted to Symposium H: Superconductivity, Materials Research Society Fall Meeting, Nov. 29–Dec. 3, 1993.

D. K. Christen, J. E. Tkaczyk, and J. M. Phillips,[1] "Electrical Transport Dissipation and Flux Pinning in Superconducting Films with Columnar Defects," abstract submitted to Symposium H: Superconductivity, Materials Research Society Fall Meeting, Nov. 11–Dec. 12, 1993.

D. M. Kroeger, A. Goyal, E. D. Specht, and Z. L. Wang,[1] and J. E. Tkaczyk and J. A. DeLuca,[10] "Evidence of Local Texture in High J_c Tl-1223 Spray Pyrolyzed Deposits," paper submitted to *Appl. Phys. Lett.* (1993).

R. A. Hawsey[1] and J. G. Daley,[16] "The Team Sport of Technology Transfer: Spectators Welcome," *Superconductor Industry* magazine, summer 1993.

S. W. Schwenterly and L. Dresner,[1] "Simple Estimate of Stored Energy and Conductor Insulation Voltage-Withstand Requirements for Advanced Solenoid Magnet Designs," presented at the CEC/ICMC, Albuquerque, N.M., July 13, 1993.

L. Dresner,[1] "Stability of an Uncooled Segment of High-Temperature Superconductor," presented at the CEC/ICMC, Albuquerque, N.M., July 13, 1993.

J. W. Lue, S. W. Schwenterly, M. S. Lubell, and J. N. Luton,[1] and C. H. Joshi, L. J. Masur, and E. R. Podtburg,[12] "Test Results of Two High Temperature Superconducting Sample Coils," presented at the CEC/ICMC, Albuquerque, N.M., July 15, 1993.

D. K. Christen and J. R. Thompson,[1] "Current Problems at High T_c," *Nature* **364** (July 8, 1993).

M. Paranthaman, J. R. Thompson, Y. R. Sun, and J. Brynestad,[1] "Synthesis and Magnetic Characterization of the High-T_c Superconducting Compound $HgBa_2CuO_{4+\delta}$," *Physica C* **213**(3 and 4) (Aug. 15, 1993).

L. Dresner,[1] "Stability and Protection of Ag/BSCCO Magnets Operated in the 20–40 K Range," *Cryog.* **33**(9) (September 1993).

E. D. Specht, A. Goyal, D. M. Kroeger, and Z. L. Wang,[1] and J. E. Tkaczyk and J. A. DeLuca,[10] *X-ray Microdiffraction Analysis of Millimeter-Scale Texture in $TlBa_2Ca_2Cu_3O_x$ Deposits*, accepted for publication in *Physica C* (1994).

L. Civale, L. Krusin-Elbaum, and F. Holtzberg,[4] and J. R. Thompson,[1] "Collective Creep of Vortex Bundles in $YBa_2Cu_3O_7$ Crystals," submitted to *Phys. Rev. Lett.* (1993).

D. M. Kroeger, A. Goyal, E. D. Specht, Z. L. Wang,[1] J. E. Tkaczyk, J. A. Sutliff, and J. A. DeLuca,[10] "The Path for Long-Range Conduction in High J_c $TlBa_2Cu_3O_{8+x}$ Spray-Pyrolyzed Deposits," presented at the TMS Fall 1993 Meeting; to be published in symposium proceedings.

W. B. Carter, G. W. Book, and A. T. Hunt,[17] "Combustion Chemical Vapor Deposition of $YBa_2Cu_3O_x$,"presented at the European Conference on Applied Superconductivity '93, held in Göttingen, Germany, October 1993; to be published in the proceedings.

M. Paranthaman, J. Brynestad, D. K. Christen, P. M. Martin, R. K. Williams, and D. M. Kroeger,[1] Y. R. Sun,[3] and J. G. Ossandon,[18] "Synthesis and Magnetic Properties of Hg-Ba-Ca-Cu-O Superconductors," abstract submitted to the Materials Research Society Spring Meeting, San Francisco, April 4–8, 1994.

D. M. Kroeger, A. Goyal, E. D. Specht, and Z. L. Wang,[1] and J. A. DeLuca, J. E. Tkaczyk, and J. Sutliff,[10] "Colony Microstructure and the Path for Strongly Linked Current Flow in Tl-1223 Deposits," abstract submitted to the Materials Research Society Spring Meeting, San Francisco, April 4–8, 1994.

R. W. Dull,[19] and H. R. Kerchner,[1] *A Teacher's Guide to Superconductivity for High School Teachers*, ORNL/M-3063, Martin Marietta Energy Systems, Oak Ridge National Laboratory, October 1993.

Z. L. Wang, R. Kontra, D. M. Kroeger, A. Goyal, and R. K. Williams,[1] "Interface and Grain Boundary Chemical Structures in YBCO Materials," submitted to *Interface Science J.* (1993).

H. Zhang, D. F. Lee, C. S. Partsinevelos, and K. Salama,[13] and V. Selvamanickam,[1] "Critical Current Dependence on Deformation Kinetics in Textured $YBa_2Cu_3O_x$ Superconductors," submitted to *J. Mater. Res.* (1993).

A. Goyal, D. M. Kroeger, E. D. Specht, and Z. L. Wang,[1] "Dependence of Critical Current Density on Microstructure in High-T_c Superconductors," abstract submitted to 1994 TMS Spring Meeting, San Francisco, Feb. 27–Mar. 3, 1994.

C. L. Briant, J. A. DeLuca, and P. Karas,[10] and A. Goyal and D. M. Kroeger,[1] "The Microstructural Evolution of Silver-Containing Spray Deposited 1223 Tl-Ca-Ba-Cu Oxide Superconductor," abstract submitted to TMS Annual Meeting, San Francisco, Feb. 27–Mar. 3, 1994.

G. N. Riley and L. Riester,[12] and A. Goyal and D. M. Kroeger,[1] "Anisotropic Elastic Modulus and Hardness of Well-Aligned Bi-2223 and Bi-2212 Powder-in-Tube Materials," abstract submitted to 1994 TMS Annual Meeting, San Francisco, Feb. 27–Mar. 3, 1994.

J. D. Budai, D. P. Norton, D. K. Christen, R. Feenstra, Q. He, B. C. Chakoumakos, E. C. Jones,[1] and R. T. Young,[5] "In-Plane Alignment of YBaCuO Films on Metal Substrates and Buffer Layers," paper presented to 1993 Materials Research Society Fall Meeting, Boston, Mass.

L. Civale, L. Krusin-Elbaum, R. Wheeler, A. D. Marwick, M. A. Kirk,[4] Y. R. Sun,[3] F. Holtzberg, and C. Field,[4] and J. R. Thompson,[1] "Arresting Vortex Motion in YBaCuO Crystals with Splay in Columnar Defects," paper submitted to *Nature* (1993).

M. Paranthaman,[1] "Single Step Synthesis of Bulk $HgBa_2Ca_2Cu_3O_{8+\delta}$ Superconductors," paper submitted to *Physica C* (1993).

G. Cui, J. Zhang, C. P. Beetz, J. Steinbeck, Z. L. Wang, and D. M. Kroeger,[1] "Epitaxial Growth of $YBa_2Cu_3O_{7-\delta}/BaTiO_3$ Thin Film Heterstructures by Magnetron Sputtering," abstract submitted to Materials Research Society Spring Meeting, San Francisco, 1994.

M. Paranthaman, Y. R. Sun, and J. R. Thompson,[1] "Synthesis and Magnetic Characterization of Bulk $HgBa_2CuO_{4+\delta}$, $HgBa_2CaCu_2O_{6+\delta}$, and $HgBa_2Ca_2Cu_3O_{8+\delta}$ Superconductors," abstract submitted to American Physical Society March Meeting, Pittsburgh, 1994.

J. R. Thompson, J. G. Ossandon, D. K. Christen, B. C. Chakoumakos, Y. R. Sun, M. Paranthaman, and J. Brynestad,[1] "Vortex Fluctuations, Magnetic Penetration Depth, and HC_2 in Hg- and Tl-Based High-T_c Superconductors," *Phys. Rev. B* **48**(18) (Nov. 1, 1993).

J. R. Thompson, D. Paul, Z. L. Wang, Z. R. Sun, D. K. Christen, H. R. Kerchner, Y. J. Chen, B. C. Sales, B. C. Chakoumakos,[1] L. Civale, L. Krusin-Elbaum, A. D. Marwick and F. Holtzberg,[4] "Enhanced Vortex Pinning and Current Density in High-T_c Materials via Tailored Defects," paper presented at Sixth U.S.-Japan Joint Workshop on Superconductivity, University of Houston, December 6, 1993.

J. A. DeLuca, P. L. Karas, C. L. Briant, and J. E. Tkaczyk[10] and A. Goyal,[1] "Progress in the Development of the Silver-Addition Process for Preparing Textured '1223' Tl-Ca-Ba-Cu-Oxide Thick Films," presented at TMS fall meeting, Pittsburgh, Pa., October 1993.

H. A. Blackstead and D. B. Pulling[20] and M. Paranthaman and J. Brynestad,[1] "Field and Temperature Dependent Surface Resistance of Superconducting Polycrystalline Multiple-Phase Hg-Ba-Ca-Cu-O: Evidence for 'Dirty-Limit' Behavior," paper submitted to *Phys. Rev. B* (1993).

C. K. Subramaniam and A. B. Kaiser[21] and M. Paranthaman,[1] "Thermoelectric Power and Resistivity of Bulk $HgBa_2CuO_{4+y}$ Superconductors and the Effects of Annealing," paper submitted to *Physica C* (1993).

J. R. Thompson, D. Paul, Z. L. Wang, D. K. Christen, H. R. Kerchner, B. C. Sales, and B. C. Chakoumakos,[1] Y. R. Sun and Y. J. Chen,[3] and L. Civale, L. Krusin-Elbaum, A. C. Marwick, and F. Holtzberg,[4] "Enhanced Vortex Pinning and Current Density in High-T_c Materials via Tailored Defects," in *Proceedings of the Sixth Annual U.S.-Japan Joint Workshop on Superconductivity*, ed. K. Salama, World Scientific, 1993.

V. Selvamanickam, A. Goyal, and D. M. Kroeger,[1] "A New Process to Texture Bulk $YBa_2Cu_3O_x$ Superconductor," paper submitted to *Appl. Phys. Lett.* (1994).

D. M. Kroeger, A. Goyal, E. D. Specht, and Z. L. Wang,[1] and J. A. DeLuca, and J. E. Tkaczyk, and J. Sutliff,[10] "Local Texture and Percolative Paths for Long-Range Conduction in High Critical Current Density $TlBa_2Ca_2Cu_3O_{8+x}$ Deposits," *Appl. Phys. Lett.* **64**(1), 106-108 (Jan 3, 1994).

G. Stejic, A. Gurevich, E. Kadyrov, R. Joynt, and D. C. Larbalestier[22] and D. K. Christen,[1] "The Effect of Geometry on the Critical Currents of Thin Films," paper submitted to *Phys. Rev. B* (1994).

L. Dresner,[1] "Quench Energies of Uncooled Superconductors," *Cryogen.* **34**(1), 77-82 (1994).

L. Dresner, "On the Connection Between Normal Zone Voltage and Hot Spot Temperature in Uncooled Magnets," *Cryogen.* **34**(2), 111-18 (1994).

L. J. Masur, E. R. Podtburg, C. A. Craven, and A. Otto,[12] Z. L. Wang and D. M. Kroeger,[1] J. Y. Coulter and M. P. Maley,[24] "Bi-axial Texture in $Ca_{0.1}Y_{0.9}Ba_2Cu_4O_8$ Composite Wires Made by Metallic Precursors," paper submitted to *Physica C* (1993).

R. A. Hawsey,[1] *ORNL Superconducting Technology Program for Electric Energy Systems. Annual Report for FY 1992*, ORNL/HTSPC-4, Martin Marietta Energy Systems, Oak Ridge National Laboratory, Feb. 2, 1993.

B. W. McConnell[1] and R. J. Ferraro,[25] *Understanding Superconducting Magnetic Energy Storage (SMES) Technology, Applications, and Economics, for End-Use Workshop*, ORNL/SUB/88-SM362/1, Martin Marietta Energy Systems, Oak Ridge National Laboratory, June 6, 1993.

S. W. Schwenterly, J. W. Lue, M. S. Lubell, and J. N. Luton,[1] and C. H. Joshi,[12] "Critical Current Measurements on an Ag/Bi-Pb-Sr-Ca-Cu-O Composite Coil as a Function of Temperature and External Magnetic Field," *IEEE Trans. Appl. Superconduct.* **3**(1), 949-52 (1993).

D. M. Kroeger and A. Goyal,[1] "Critical Currents and Microstructures in Oxide Superconductors, *JOM*, Oct., 42-47 (1992).

D. M. Kroeger,[1] *Report of Foreign Travel, November 6-20, 1992*, ORNL/FTR-4507, Martin Marietta Energy Systems, Oak Ridge National Laboratory, Dec. 12, 1992.

Z. L. Wang, A. Goyal, D. M. Kroeger,[1] and T. Armstrong,[26] "Defects Near the $Y_2BaCuO_5/YBa_2Cu_3O_{7-x}$ Interface and Their Effect on Flux-Pinning in Melt Processed and Quench-Melt-Growth Processed $YBa_2Cu_3O_{7-x}$," pp. 181-86 in *Proceedings of the Spring Meeting, Materials Research Society, San Francisco, Apr. 27-May 1, 1992*, Mater. Res. Soc., Pittsburgh, 1992.

Z. L. Wang, R. Kontra, A. Goyal, D. M. Kroeger, and L. F. Allard,[1] "Flux-Pinning - Related Defect Structures in Melt-Processed $YBa_2Cu_3O_{7-x}$, pp. 936-37 in *Proceedings 51st Annual Meeting, Microsc. Society of America, Cincinnati, Aug. 1-6, 1993*, San Francisco Press, 1993.

Z. L. Wang, J. Brynestad, R. K. Williams, and D. M. Kroeger,[1] Y. R. Sun,[3] and J. R. Thompson,[1,3] "Nano-Probe Microanalysis of Grain Boundary Chemistry in $YBa_2Cu_4O_8$ and Its Relationship to Weak-Link Behavior," pp. 598-99 in *Proceedings 51st Annual Meeting Microsc. Society of America, Cincinnati, Aug. 1-6, 1993*, San Francisco Press, 1993.

Z. L. Wang, A. Goyal, and D. M. Kroeger,[1] "Structural and Chemical Disorder Near the $Y_2BaCuO_5/YBa_2Cu_3O_{7-\delta}$ Interface and Its Possible Relation to the Flux-Pinning Behavior in Melt-Textured $YBa_2Cu_3O_{7-\delta}$," *Phys. Rev. B* **47**(9), 5373-82 (1993).

J. D. Budai,[1] R. T. Young,[5] and B. S. Chao,[5] "In-Plane Epitaxial Alignment of $YBa_2Cu_3O_{7-y}$ Films Grown on Silver Crystals and Buffer Layers," *Appl. Phys. Lett.* **62**(15), 1836-38 (1993).

J. R. Thompson,[1,3] D. K. Christen, H. R. Kerchner, B. C. Sales, and B. C. Chakoumakos,[1] and L. Civale, A. D. Marwick, and F. Holtzberg,[4] "Limits to Critical Currents in High-Temperature Superconductors: What We Can Learn from Tailored Defects," pp. 24-36 in *Proceedings 6th Annual Conference on Superconductivity and Its Implications, Buffalo, N.Y., Sept. 15-17, 1992*, Am. Inst. Phys., New York, 1992.

J. R. Thompson,[1,3] and M. A. Kirk, R. Wheeler,[4] L. Civale, T. K. Worthington, L. Krusin-Elbaum, A. D. Marwick, and F. Holtzberg,[4] "Irradiation-Enhanced Pinning in $YBa_2Cu_3O_{7-x}$ Crystals," *JOM* Oct., 60-64 (1992).

R. Feenstra, D. P. Norton, J. D. Budai, D. K. Christen, D. H. Lowndes, V. C. Matijasevic, C. B. Eom, T. H. Geballe, E. S. Hellman, and E. H. Hartford, "T_c-Delta Relations in $YBa_2Cu_3O_{7-\delta}$ Thin Films: Effects of Oxygen Pressure During Growth," pp. 101-6 in *Proceedings Spring Meeting Materials Research Society, San Francisco, Apr. 27-May 1, 1992*, Mater. Res. Soc., Pittsburgh, 1992.

Y. R. Sun,[3] J. R. Thompson,[1,3] and Y. J. Chen, D. K. Christen, and A. Goyal,[1] "Strong Evidence for Vortex-Glass-Collective-Pinning Theory in $YBa_2Cu_3O_7$ Superconductors," *Phys. Rev. B* **47**(21), 14481-88 (1993).

J. R. Thompson,[1,3] Y. R. Sun,[3] J. G. Ossandon, D. K. Christen, H. R. Kerchner, B. C. Sales, and B. C. Chakoumakos,[1] and L. Civale, A. D. Marwick, and F. Holtzberg,[4] "Magnetic Studies of Current Conduction and Flux Pinning in High-T_c Cuprates: Virgin, Irradiated, and Oxygen Deficient Materials," pp. 179-88 in *Proceedings New York State Conference on Superconductivity and Applications, Buffalo, N.Y., Sept. 15-17, 1992*, Am. Inst. Phys., New York, 1993.

J. R. Thompson,[1,3] Y. R. Sun,[3] J. G. Ossandon, D. K. Christen, H. R. Kerchner, B. C. Sales, and B. C. Chakoumakos,[1] and L. Civale, A. D. Marwick, and F. Holtzberg,[4] "Magnetization and Flux Pinning in High-T_c Cuprates: Virgin, Irradiated and Oxygen Deficient Materials," pp. 232-36 in *Proceedings 5th U.S./Japan Workshop on High T_c Superconductors, Tsukuba, Japan, Nov. 9-10, 1992*, Soc. Nontraditional Technol., Tokyo, 1993.

J. E. Tkaczyk, J. A. DeLuca, P. L. Karas, and P. J. Bednarczyk,[10] and D. K. Christen, C. E. Klabunde, and H. R. Kerchner,[1] "Enhanced Transport Critical Current at High Fields after Heavy Ion Irradiation of Textured $TlBa_2Ca_2Cu_3O_z$ Thick Films," *Appl. Phys. Lett.* **62**(23), 3031-33 (1993).

S. Zhu, D. K. Christen, C. E. Klabunde, J. R. Thompson, E. C. Jones, R. Feenstra, D. H. Lowndes, and D. P. Norton, "Superconducting Transport Properties of Epitaxial $YBa_2Cu_3O_{7-\delta}$ Thin Films: A Consistent Description Based on Thermally Activated Flux Motion," *Phys. Rev. B* **46**(9), 5576-80 (1992).

---

1. Oak Ridge National Laboratory.
2. Westinghouse Electric Corporation.
3. University of Tennessee.
4. International Business Machines.
5. Energy Conversion Devices, Incorporated.
6. SUNY at Buffalo.
7. Argonne National Laboratory.
8. University of Illinois.
9. Northern Illinois University.
10. General Electric Corporate Research and Development.
11. University of Rochester.
12. American Superconductor Corporation.
13. Texas Center for Superconductivity, University of Houston.
14. University of Colorado.
15. Dow Chemical Company.
16. U.S. Department of Energy Headquarters.
17. Georgia Institute of Technology.
18. University of Talca, Chile.
19. Largo High School.

20. University of Notre Dame.
21. Victoria University of Wellington.
22. University of Wisconsin.
23. National Institute of Science and Technology.
24. Los Alamos National Laboratory.
25. Ferraro, Oliver, & Associates, Inc.
26. Pacific Northwest Laboratory.

INTERNAL DISTRIBUTION

1. J. D. Budai
2. R. S. Carlsmith
3. D. K. Christen
4. D. F. Craig
5. L. Dresner
6. L. B. Dunlap
7. W. Fulkerson
8. A. Goyal
9–18. R. A. Hawsey
19. D. R. James
20. C. J. Janke
21. D. M. Kroeger
22. R. J. Lauf
23. F. A. List
24. M. S. Lubell
25. D. H. Lowndes
26. J. W. Lue
27. B. W. McConnell
28. J. W. McKeever
29. R. W. Murphy
30. D. P. Norton
31. W. P. Painter
32. M. Paranthaman
33. J. B. Roberto
34. A. C. Schaffhauser
35. S. W. Schwenterly
36. V. Selvamanickam
37. J. Sheffield
38. V. K. Sikka
39. J. P. Stovall
40. J. R. Thompson
41–43. J. W. Turner
44. R. K. Williams
45–46. Laboratory Records Dept.
47. Laboratory Records—RC
48. Central Research Library
49. ORNL Patent Office

EXTERNAL DISTRIBUTION

50. U. Balachandran, Argonne National Laboratory, ET/212, 9700 South Cass Avenue, Argonne, Illinois 60439-4838
51. D. O. Welch, Brookhaven National Laboratory, Materials Science Division, Upton, Long Island, New York 11973
52. C. Matzdorf, Energetics, Inc., 7164 Columbia Gateway Drive, Columbia, Maryland 21046
53. D. E. Peterson, Los Alamos National Laboratory, Superconductivity Technology Center, Mail Stop K763, Los Alamos, New Mexico 87564.
54. R. D. McConnell, National Renewable Energy Laboratory, 1617 Cole Boulevard, Golden, Colorado 80401
55. T. C. Bickel, Sandia National Laboratories, MS 0752, P. O. Box 5800, Albuquerque, New Mexico 87185-0752
56. J. G. Daley, EE-142/FORS, U.S. Department of Energy, Advanced Utility Concepts Division, Office of Energy Management, 6H-034, 1000 Independence Avenue, S.W., Washington, D.C. 20585
57. R. Eaton, EE-142/FORS, U.S. Department of Energy, Advanced Utility Concepts Division, Office of Energy Management, 6H-034, 1000 Independence Avenue, S.W., Washington, D.C. 20585

58. M. E. Gunn, Jr., EE-14/FORS, U.S. Department of Energy, Office of Energy Management, 6H-034, 1000 Independence Avenue, S.W., Washington, D.C. 20585
59. H. E. Clark, U.S. Department of Energy, Office of Assistant Manager for Energy Research and Development, Oak Ridge Field Office, P.O. Box 2008, Oak Ridge, Tennessee 37831-6269
60-61. U.S. Department of Energy, Office of Scientific and Technical Information, P.O. Box 62, Oak Ridge, Tennessee 37831-0062
62. G. J. Yurek, American Superconductor Corporation, Two Technology Drive, Westborough, Massachusetts 01581
63. C. B. Zimm, Astronautics Corporation of America, Technology Center, 5800 Cottage Grove Road, Madison, Wisconsin 53716-1387
64. M. V. Parish, CeraNova Corporation, P.O. Box 278, Hopkinton, Massachusetts 01748-0278
65. Paul Grant, Electric Power Research Institute, P.O. Box 10412, Palo Alto, California 94303
66. J. W. Bray, General Electric Corporate Research and Development, Building K-1, Room 1C25, P.O. Box 8, Schenectady, New York 12301
67. C. H. Rosner, Intermagnetics General Corporation, 450 Old Niskayuna Road, Latham, New York 12110
68. K. R. Marken, Jr., Oxford Superconducting Technology, P.O. Box 429, Carteret, New Jersey 07008-0429
69. M. J. Tomsic, Plastronic, Inc., 35 Marybill Drive, Troy, Ohio 45373
70. J. W. Locher, Saphikon, Inc., 33 Powers Street, Milford, New Hampshire 03055
71. D. C. Larbalestier, University of Wisconsin-Madison, Applied Superconductivity Center, 1500 Johnson Drive, Madison, Wisconsin 53706
72. C. C. Tsuei, IBM Research Division, T. J. Watson Research Center, P.O. Box 218, Yorktown Heights, New York 10598

DATE
FILMED
7/01/94
END